Journal for ImmunoTherapy of Cancer

Precision enhancement of CAR-NK cells through non-viral engineering and highly multiplexed base editing

Minjing Wang ,[1,2,3,4] Joshua B Krueger ,[1,2,3] Alexandria K Gilkey,[1,2,3] Erin M Stelljes,[1,2,3] Mitchell G Kluesner,[1,2,3] Emily J Pomeroy,[1,2,3] Joseph G Skeate ,[1,2,3] Nicholas J Slipek,[1,2,3] Walker S Lahr,[1,2,3] Patricia N Claudio Vázquez,[1,2,3,4] Yueting Zhao,[1,2,3] Jason B Bell ,[1,2,3] Kendell Clement ,[5] Ella J Eaton,[1,2,3,4] Kanut Laoharawee,[1,2,3,4] Jae-Woong Chang,[1,2,3] Beau R Webber,[1,2,3] Branden S Moriarity[1,2,3]

To cite: Wang M, Krueger JB, Gilkey AK, *et al*. Precision enhancement of CAR-NK cells through non-viral engineering and highly multiplexed base editing. *Journal for ImmunoTherapy of Cancer* 2025;**13**:e009560. doi:10.1136/jitc-2024-009560

► Additional supplemental material is published online only. To view, please visit the journal online (https://doi.org/10.1136/jitc-2024-009560).

Accepted 20 March 2025

For numbered affiliations see end of article.

Correspondence to
Branden S Moriarity; mori0164@umn.edu

Dr Beau R Webber; webb0178@umn.edu

ABSTRACT

Background Natural killer (NK) cells' unique ability to kill transformed cells expressing stress ligands or lacking major histocompatibility complexes (MHC) has prompted their development for immunotherapy. However, NK cells have demonstrated only moderate responses against cancer in clinical trials.

Methods Advanced genome engineering may thus be used to unlock their full potential. Multiplex genome editing with CRISPR/Cas9 base editors (BEs) has been used to enhance T cell function and has already entered clinical trials but has not been reported in human NK cells. Here, we report the first application of BE in primary NK cells to achieve both loss-of-function and gain-of-function mutations.

Results We observed highly efficient single and multiplex base editing, resulting in significantly enhanced NK cell function in vitro and in vivo. Next, we combined multiplex BE with non-viral *TcBuster* transposon-based integration to generate interleukin-15 armored CD19 chimeric antigen receptor (CAR)-NK cells with significantly improved functionality in a highly suppressive model of Burkitt's lymphoma both in vitro and in vivo.

Conclusions The use of concomitant non-viral transposon engineering with multiplex base editing thus represents a highly versatile and efficient platform to generate CAR-NK products for cell-based immunotherapy and affords the flexibility to tailor multiple gene edits to maximize the effectiveness of the therapy for the cancer type being treated.

WHAT IS ALREADY KNOWN ON THIS TOPIC

⇒ Cancer immunotherapy using primary natural killer (NK) cells has demonstrated an outstanding safety profile clinically but limited efficacy in treating malignancies.

⇒ Engineering primary NK cells with CRISPR/Cas9 and viruses poses safety concerns.

WHAT THIS STUDY ADDS

⇒ First application of base editing (BE) technology in primary human NK cells with high efficiency at both single and multiplex level with minimum safety concerns.

⇒ First installation of non-cleavable CD16a to enhance ADCC in NK cells through base editing.

⇒ First report of using *TcBuster* and BE contemporaneously in manufacturing primary chimeric antigen receptor-NK cells.

HOW THIS STUDY MIGHT AFFECT RESEARCH, PRACTICE OR POLICY

⇒ This study creates a highly flexible and efficient engineering platform for tailored NK-based cell therapy against various types of cancer.

⇒ The fully non-viral approach described in this study represents a highly efficient, safe and cost-effective option for the manufacture of NK-based cell therapy products.

INTRODUCTION

Natural killer (NK) cells have garnered extensive attention in immunotherapy due to their unique ability to kill transformed cells lacking major histocompatibility complexes (MHC) and antibody-bound target cells through antigen-dependent cellular cytotoxicity (ADCC). From simply infusing allogeneic donor NK cells for treating hematological malignancies[1] to adoptive therapy harnessing NK cells with chimeric antigen receptor (CAR) for a wide range of solid tumors, NK cells have exhibited many advantages over T cell-based therapy.[2] Despite promising early outcomes in clinical studies, rarely have NK cell therapies led to durable complete remission or tumor clearance.[3 4] Extensive studies have pointed to NK cell dysfunction, exhaustion, and lack of persistence as major contributing factors to the modest clinical outcomes.[5]

To date, engineering NK cells to express CAR constructs has relied almost exclusively

on viral transduction with retroviruses and recombinant adeno-associated virus.[6] Although highly efficient at delivering CAR constructs into NK cells, virus cargo size limits and the risk of insertional oncogenesis present major drawbacks for clinical applications.[6] Comparatively, DNA transposon systems, including *Sleeping Beauty, PiggyBac*, and *TcBuster*, are less restricted by cargo size and afford a more economical and expeditious path to clinical manufacturing of CAR-NK cells.[7–10] Moreover, transposon systems allow for stable gene transfer in NK cells, which has distinct advantages over other non-viral systems, such as transient messenger RNA (mRNA) transfection.[6]

Limited *in vivo* persistence and durability issues in the absence of cytokine support are major challenges to effective NK-based immunotherapy.[11] Notably, NK cell persistence, metabolic fitness, and functionality have been enhanced through supplementation with exogenous interleukin (IL)-15 or IL-2 in vitro and in vivo,[12–17] suggesting gamma chain cytokine support may be a prerequisite to successful NK-based immunotherapies.[11 18] To this end, some NK-based clinical trials tested continuous intravenous infusion of IL-15 to maintain NK cell persistence; however, this costly and toxic approach has driven researchers to develop IL-15 expressing NK cells, that is, cytokine armored NK cells.[18–21] In fact, recent preclinical and clinical studies have demonstrated successful expression of soluble IL-15 (sIL-15) in CAR-NK cells using retroviral engineering, which led to improved cytotoxicity and persistence *in vivo*.[20–22]

Beyond cytokine armoring, we[23] and others[24–27] have demonstrated that CRISPR/Cas9 can be used to enhance NK cell function through targeted gene knockout (KO). However, this approach is not ideal for multiplex gene KO as translocations and other genomic rearrangements can occur due to simultaneous induction of multiple double-strand breaks (DSBs). Due to these concerns, we previously deployed base editor (BE) technology in primary human T cells to enhance CAR-T cell function through multiplex gene KO.[28] BEs consist of a catalytically inactive Cas9 fused to a deaminase domain for site-specific nucleotide base conversion, allowing users to install gain or loss of function mutations without induction of a DSB or requirement for a DNA donor molecule.[29–32] However, BEs have yet to be deployed for primary NK cell engineering to achieve similar multiplex base editing.

Here, we report the first highly efficient engineering of NK cells using an adenine BE (ABE), ABE8e,[33] to achieve both loss-of-function and gain-of-function mutations in NK cells to improve their function. We also explored the upper limit of simultaneous multiplex base editing and observed no significant reduction in base editing efficiency targeting up to six independent loci. Next, we identified optimal, synergistic multiplex KO combinations and codelivered a CD19 CAR and IL-15 armoring using the *TcBuster* DNA transposon system to develop a non-viral engineered CAR-NK cell product tailored specifically to overcome a highly suppressive model of Burkitt's lymphoma. Our work serves as proof of concept that precision enhancement of CAR-NK cells can be achieved using simultaneous multiplex base editing and non-viral transposon-based engineering to generate CAR-NK therapies tailored for user-defined cancer types.

RESULTS

Highly efficient single gene KO in primary human NK cells using ABE

BEs are capable of highly efficient gene KO without double-stranded break induction through splice site disruption or installations of stop codons.[28 34–38] We first examined whether single gene KO could be achieved using BE in primary NK cells and evaluated consequent changes in immune function. Given that suppression of inhibitory signals is one of the most common strategies for enhancing NK-based therapy,[39] we assembled a panel of targets focusing largely on intracellular and extracellular inhibitory proteins expressed by NK cells (table 1). Intracellular checkpoints include aryl hydrocarbon receptor

Table 1 List of genes for KO in NK cells using BE

Gene name	Protein name	Subcellular location	Functions in NK cell	sgRNA sequence
AHR	Aryl hydrocarbon receptor (AhR)	Intracellular	Positive regulator of CD56 expression in NK cells	CTTACCATCAAAGAAGCTCT
CISH	Cytokine-inducible SH2-containing protein (CIS)	Intracellular	Negative regulator of IL-15 signaling in NK cells	CTCACCAGATTCCCGAAGGT
TIGIT	T cell immunoreceptor with Ig and ITIM domains	Cell Membrane	Immune checkpoint in NK cells leads to cell exhaustion	CAGGCCTTACCTGAGGCGAG
KLRG1	Killer cell lectin-like receptor subfamily G member 1	Cell Membrane	Inhibitory receptor on NK cell surfaces	CCTTACCTTGAGAAGTTTAG
PDCD1	Programmed cell death protein 1 (PD-1/CD279)	Cell Membrane	Immune checkpoint in NK cells that plays a role in immunosuppression	CACCTACCTAAGAACCATCC

BE, base editor; IL-15, interleukin-15; KO, knockout; NK, natural killer.

(*AHR*), a negative regulator of NK cell cytotoxicity when agonists (ie, kynurenine) are present in the tumor microenvironment (TME),[40] and cytokine-inducible SH2-containing protein (*CISH*), a negative regulator of IL-15 signaling essential for NK cell development and function.[37] On the surface of NK cells, programmed cell death protein 1 (*PDCD1*) and T-cell immunoreceptor with Ig and ITIM domains (*TIGIT*) are well-defined inhibitory immune checkpoints whose signal blockade has been seen in a wide range of clinical applications.[41 42] Killer cell lectin-like receptor subfamily G member 1 (*KLRG1*), an emerging target in immunotherapy, is an additional inhibitory immune checkpoint with potential clinical relevance.[43] Since our previous BE studies found targeting splice donors (SD) is the most efficient method for gene disruption, we designed single guide RNAs (sgRNAs) targeting a SD in each gene of interest using SpliceR, an in-house-developed online BE sgRNA design and prediction tool.[38] Each sgRNA was co-transfected with ABE8e mRNA into feeder-stimulated peripheral blood (PB) NK cells isolated from healthy donors by electroporation. KO efficiency was then assessed at the genomic level through Sanger sequencing and quantification of A-to-G conversion rates using EditR software (figure 1A).[44] Specifically, A-to-G conversion rates for each targeted gene were as follows: *AHR* 100% (± 0%), *CISH* 99.67% (± 0.58%), *KLRG1* 65.07% (± 14.86%), *TIGIT* 100% (± 0%), *PDCD1* 86.33% (± 7.51%). Example sequencing results of each target gene as assessed by EditR are shown in online supplemental figure 1A–E.[44] Of note, indels were not detectable for any of the target genes in all three donors (online supplemental figure 2). Next, we assessed protein level KO of each target gene via western blot (WB) or flow cytometry using donor-matched control NK cells (figure 1B and online supplemental figure 3A–D). For intracellular proteins, WB analysis showed an average protein reduction of 95.60% (± 3.88%) for AhR, and 99.59% (± 0.71%) for CISH. Flow analysis demonstrated a 96.78% (± 4.41%) reduction of TIGIT surface expression, while KLRG1 showed an average of 65% (± 14.86%) reduction in protein expression. Note that PD-1 protein loss results are not shown here, as minimal detection of PD-1 was achieved in all healthy donors used. This observation is in line with previous studies reporting low *detectable* expression (<5%) of PD-1 in NK cells of healthy individuals and elevated expression in patients bearing tumors.[45–53]

We next assessed whether individual gene KOs translated into the expected functional enhancement of NK cells by designing functional assays specific for each gene target. Starting with the intracellular targets, AHR agonists are known to suppress NK cell cytotoxicity during tumor progression and metastasis.[40 54] Thus, we cultured NK cells with an AHR agonist, L-Kynurenine (L-Kyn), for two rounds of 7 day expansion (14 days) before co-culturing them with K562 target cells at various effector-to-target (E:T) ratios (figure 1C). Our results showed that L-Kyn significantly reduced NK cell killing overall, however, *AHR* KO NK exhibited significantly higher levels of killing than control NK (figure 1D,E and online supplemental figure 4A–D). Due to its role in negative regulation of IL-15 signaling, several groups reported improved functionality of NK cells with *CISH* KO.[37 55 56] Here, we co-cultured *CISH* KO and control NK cells with an aggressive acute myeloid leukemia cell line, Molm-13, for 48 hours at multiple E:T ratios (figure 1F). Compared with control NK, *CISH* KO NK exhibited enhanced cytotoxicity against Molm-13 cells, in line with previous reports (figure 1G).[37 55 56]

Next, we examined the functional impacts of surface checkpoint KOs. TIGIT/CD155 interaction serves as an inhibitory immune checkpoint in NK cells, and other studies have demonstrated enhanced NK cell cytotoxicity with *TIGIT* KO.[57–59] In line with these reports, BE-mediated *TIGIT* KO NK cells co-cultured with Raji cells engineered to overexpress CD155 (ie, Raji CD155^{hi} cells) for 48 hours at different E:T ratios exhibited significantly higher cytotoxicity against Raji CD155^{hi} cells compared with donor-matched control NK cells (figure 1H,I). Analogous to TIGIT/CD155, the PD-1/PD-L1 axis is another well-known inhibitory immune checkpoint in NK cells.[60–63] BE-mediated *PDCD1* KO NK cells co-cultured with Raji cells engineered to overexpress PD-L1 (ie, PD-L1^{hi} cells) showed enhanced killing versus control NK cells (figure 1J,K). Finally, E-cadherin (E-Cad) binding to KLRG1 has been shown to protect tumor cells from cytolysis by NK cells.[64] Thus, we co-cultured NK cells with either E-Cad(+) cells (Raji) or E-Cad(−) cells (Jurkat) and performed intracellular cytokine staining (ICS) to assess activation (figure 1L). In contrast to previous reports, we observed no significant differences in CD107a positivity and interferon-gamma (IFN-γ) expression between control NK and KLRG1 KO NK against E-Cad(+) or E-Cad(−) target cells (figure 1M,N). In summary, using ABE8e we were able to achieve highly efficient single gene KO in NK cells, which translated into *in vitro* functional enhancement against multiple tumor models, with the exception of *KLRG1* KO.

Highly efficient installation of a non-cleavable CD16A mutation in NK cells using ABE

Given that BE can target individual nucleotides to alter amino acid codons, we next sought to establish whether ABE could be used to enhance NK cell function through gain-of-function mutations. CD16a is an Fc receptor expressed on the surface of NK cells which mediates ADCC.[65] On NK cell activation, CD16a undergoes a proteolytic cleavage process by ADAM17 as a negative feedback mechanism regulating NK cell cytotoxicity (figure 2A).[66] Previous studies have found that a single amino acid substitution (S197P) at the cleavage site of ADAM17 on CD16a rendered the receptor "non-cleavable", and expression of the non-cleavable CD16a (ncCD16a) cDNA in NK cells enhanced ADCC.[67] Here, we sought to install the ncCD16a mutation at the endogenous locus using ABE8e as a proof-of-principle of

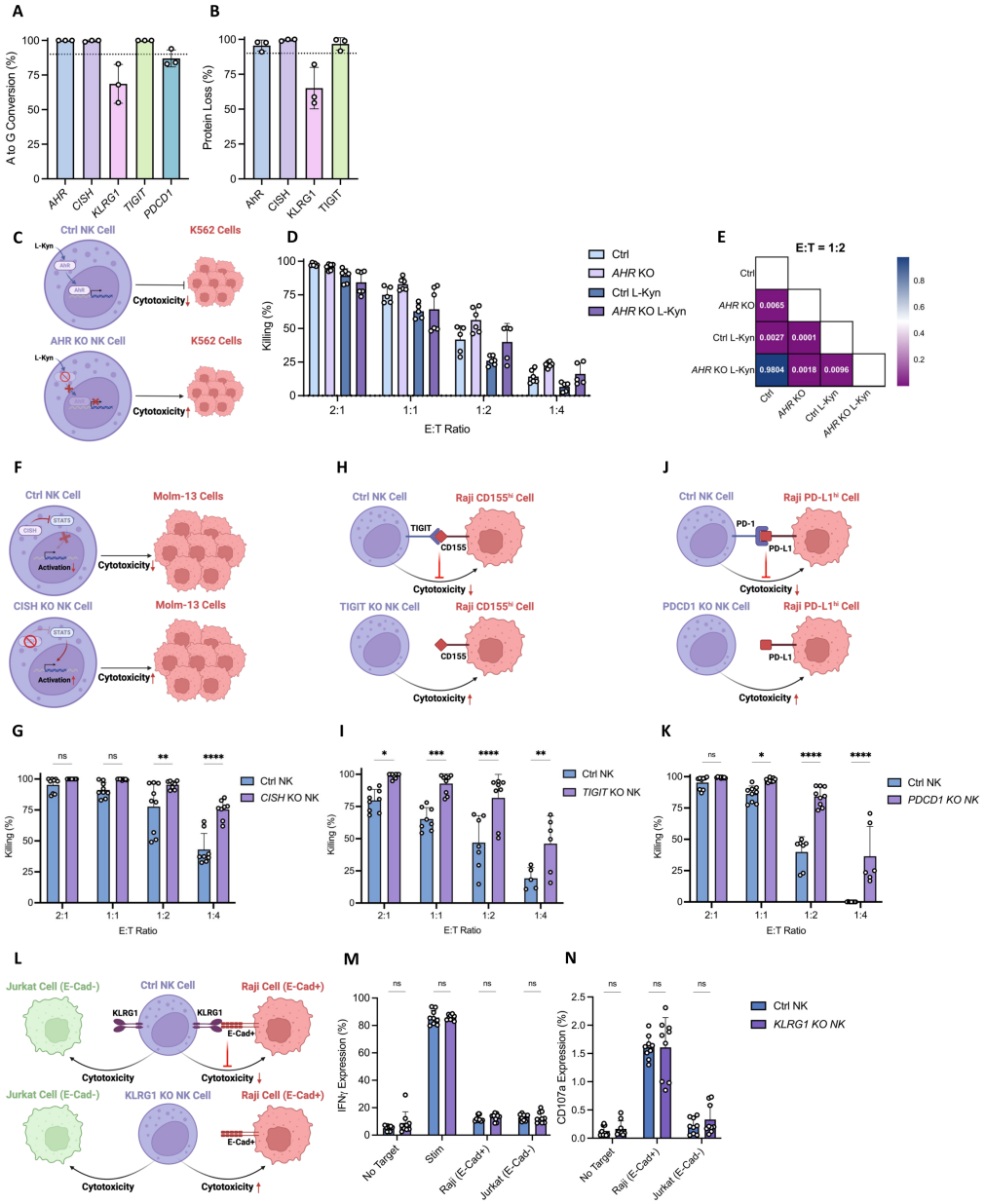

Figure 1 Highly efficient single gene KO in NK cells using BE. (A) Editing efficiency at genomic level quantified by A-to-G conversion of target base for each gene locus (n=3 independent NK cell donors). (B) Editing efficiency at protein level quantified by percentage of protein loss of each gene (n=3 independent NK cell donors). (C) Schema of killing assay to assess the functional improvement of AHR KO NK cells. (D) Ability of AHR KO versus Ctrl NK cells (with or without 14 days of L-Kynurenine pretreatment) to kill K562 cells at various E:T ratios as measured by luciferase luminescence assay. Assays run in triplicate in n=2 independent biological NK cell donors. (E) Statistical significance (p value) between each condition of AHR KO functional killing assay at E-to-T ratio of 1:2. (F) Schema of killing assay to assess the functional improvement of CISH KO NK cells. (G) Ability of CISH KO versus Ctrl NK cells to kill Molm-13 cells at various E:T ratios as measured by luciferase luminescence assay. Assays run in triplicate in n=3 independent biological NK cell donors. (H) Schema of killing assay to assess the functional improvement of TIGIT KO NK cells. (I) Ability of TIGIT KO versus Ctrl NK cells to kill Raji CD155^{hi} cells at various E:T ratios as measured by luciferase luminescence assay. Assays run in triplicate in n=3 independent biological NK cell donors. (J) Schema of killing assay to assess the functional improvement of PDCD1 KO NK cells. (K) Ability of PDCD1 KO versus Ctrl NK cells to kill Raji PD-L1^{hi} cells at various E:T ratios as measured by luciferase luminescence assay. Assays run in triplicate in n=3 independent biological NK cell donors. (L) Schema of ICS assay to assess the functional improvement of KLRG1 KO NK cells. (M) and (N) Cytokine production (M) and degranulation (N) ability of KLRG1 KO versus Ctrl NK cells against E-Cad+ Raji cells or E-Cad– Jurkat cells as measured by percentage of NK cells producing IFNγ and CD107a. Assays run in triplicate in n=3 independent biological NK cell donors. Data represented as mean±SD. P values calculated by two-way ANOVA test (n.s. p>0.05, *p≤0.05, **p≤0.01, ***p≤0.001, ****p≤0.0001). AHR, Aryl hydrocarbon receptor; ANOVA, analysis of variance; BE, base editor; CISH, cytokine-inducible SH2-containing protein; E:T, effector-to-target; ICS, intracellular cytokine staining; IFN-γ, interferon-gamma; KLRG1, killer cell lectin-like receptor subfamily G member 1; KO, knockout; NK, natural killer; PDCD1, programmed cell death protein 1; TIGIT, T cell immunoreceptor with Ig and ITIM domains.

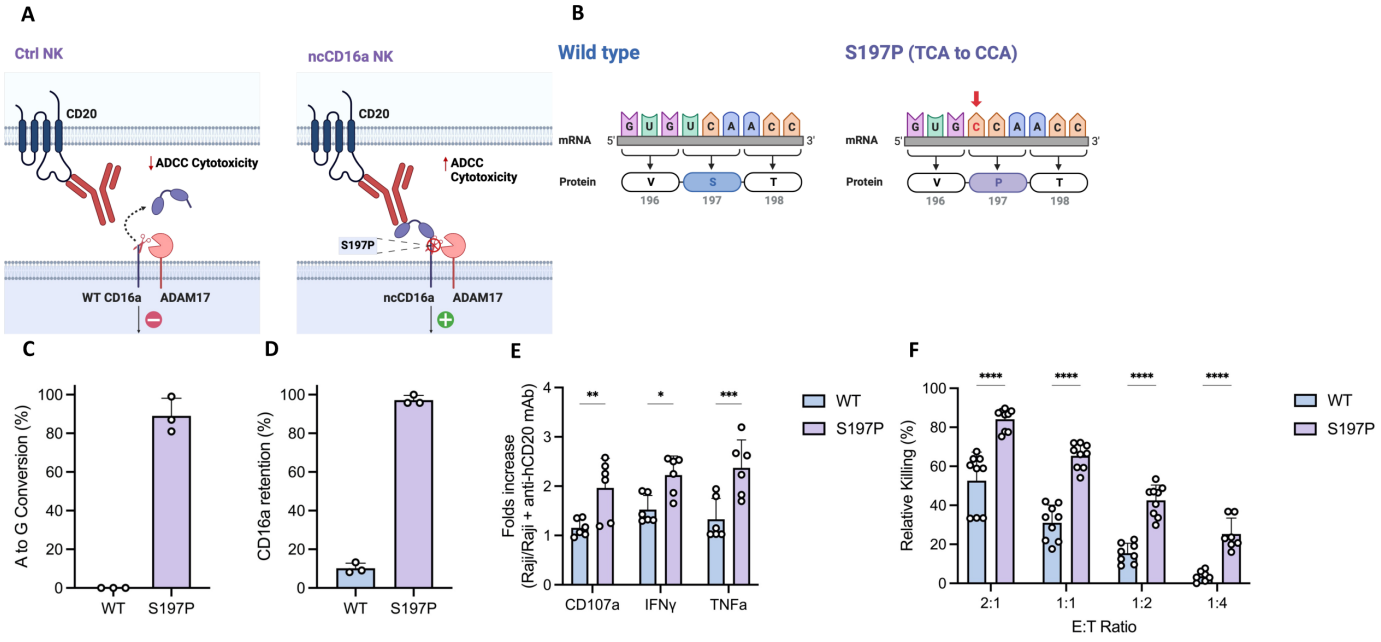

Figure 2 Highly efficient gain-of-function mutation in NK cells using BE. (A) Schema of how the S197P mutation renders NK cells non-cleavable by ADAM17 and results in enhanced ADCC cytotoxicity. (B) Schema of the recreation of S197P ncCD16a NK cells by a single base modification by BE. (C) Editing efficiency at genomic level quantified by A-to-G conversion of target base for *CD16A* (n=3 independent NK cell donors). (D) Editing efficiency at protein level quantified by CD16a retention on NK cell surface after PMA treatment (n=3 independent NK cell donors). (E) Cytokine production of S197P CD16a versus WT CD16a NK cells against CD20+Raji cells during ADCC (E:T ratio: 1:1). Plotted by folds increase of each cytokine with versus without anti-hCD20 mAb co-treatment. Assays run in duplicate in n=3 independent biological NK cell donors. (F) Ability of S197P CD16a versus WT CD16a NK cells to carry out ADCC against anti-hCD20 mAb treated CD20+Raji cells at various E:T ratios as measured by luciferase luminescence assay. Assays run in triplicate in n=3 independent biological NK cell donors. Data represented as mean±SD. P values calculated by two-way ANOVA test (*p≤0.05, **p≤0.01, ***p≤0.001, ****p≤0.0001). ADCC, antigen-dependent cellular cytotoxicity; ANOVA, analysis of variance; BE, base editor; CCA, cytosine-cytosine-adenine; E:T, effector-to-target; IFN-γ, interferon-gamma; mAb, monoclonal antibody; mRNA, messenger RNA; NK, natural killer; PMA, phorbol 12-myristate 13-acetate; TCA, thymine-cytosine-adenine WT, wild type.

ABE-based gain-of-function engineering in NK cells. To this end, we designed an sgRNA targeting serine 197 at the ADAM17 cleavage site with the goal of replicating the S197P mutation through a single A-to-G base conversion, altering the mRNA codon from uracil-cytosine-adenine (UCA) to cytosine-cytosine-adenine (CCA) (figure 2B). Sequencing results validated our prediction and yielded an average A-to-G conversion rate of 89% (± 9.17%, n=3) in NK cells with the highest conversion rate observed at 99% in one donor (figure 2C; online supplemental figure 5A). To assess whether the installation of this mutation conferred cleavage resistance, NK cells were stimulated with phorbol 12-myristate 13-acetate (PMA) to activate ADAM17 and then assessed for CD16a retention (ie, % of CD16a detected with PMA treatment vs % of CD16a detected without PMA treatment). As shown in online supplemental figure 2D and online supplemental figure 5B, we observed an average of 97.17% (± 2.45%) CD16a retention after PMA treatment in ABE8e engineered NK cells, with the highest retention rate approaching 100%.

Next, to validate the functionality of our ncCD16a NK cells, we tested their ability to mediate ADCC against Raji cells treated with an anti-hCD20-mAb. We first assessed activation of ncCD16a NK cells in this assay via ICS for degranulation (CD107a) and cytokine production (TNF-α and IFN-γ). Compared with non-engineered NK cells, ncCD16a NK cells demonstrated significantly increased CD107a, IFN-γ, and TNF-α expression when co-cultured with cell targets treated with anti-hCD20-mAb, indicating enhanced ADCC-driven activation (measured by Raji vs Raji cotreatment with anti-hCD20-mAb) of ncCD16a NK cells (figure 2E). Functionally, we assessed NK cytotoxicity via ADCC using an ADCC co-culture killing assay against Raji cells at different E:T ratios. As predicted, ncCD16a NK exhibited significantly enhanced killing of Raji cells compared with control NK cells throughout all E:T ratios tested (figure 2F). Surprisingly, when co-cultured without anti-hCD20-mAb, ncCD16a NK also demonstrated significantly enhanced killing compared with that of control NK cells (online supplemental figure 5C). Taken together, these data demonstrate that ABE is capable of installing gain-of-function mutations in NK cells at high efficiencies to improve NK cell functionality.

Highly efficient multiplex base editing in NK cells using ABE

Next generation cellular therapies will likely require a multitude of tailored gene edits to maximize efficiency, particularly when addressing hard-to-treat solid tumor cancers. Previously, our group has shown multiplex base editing can be used to enhance CAR-T

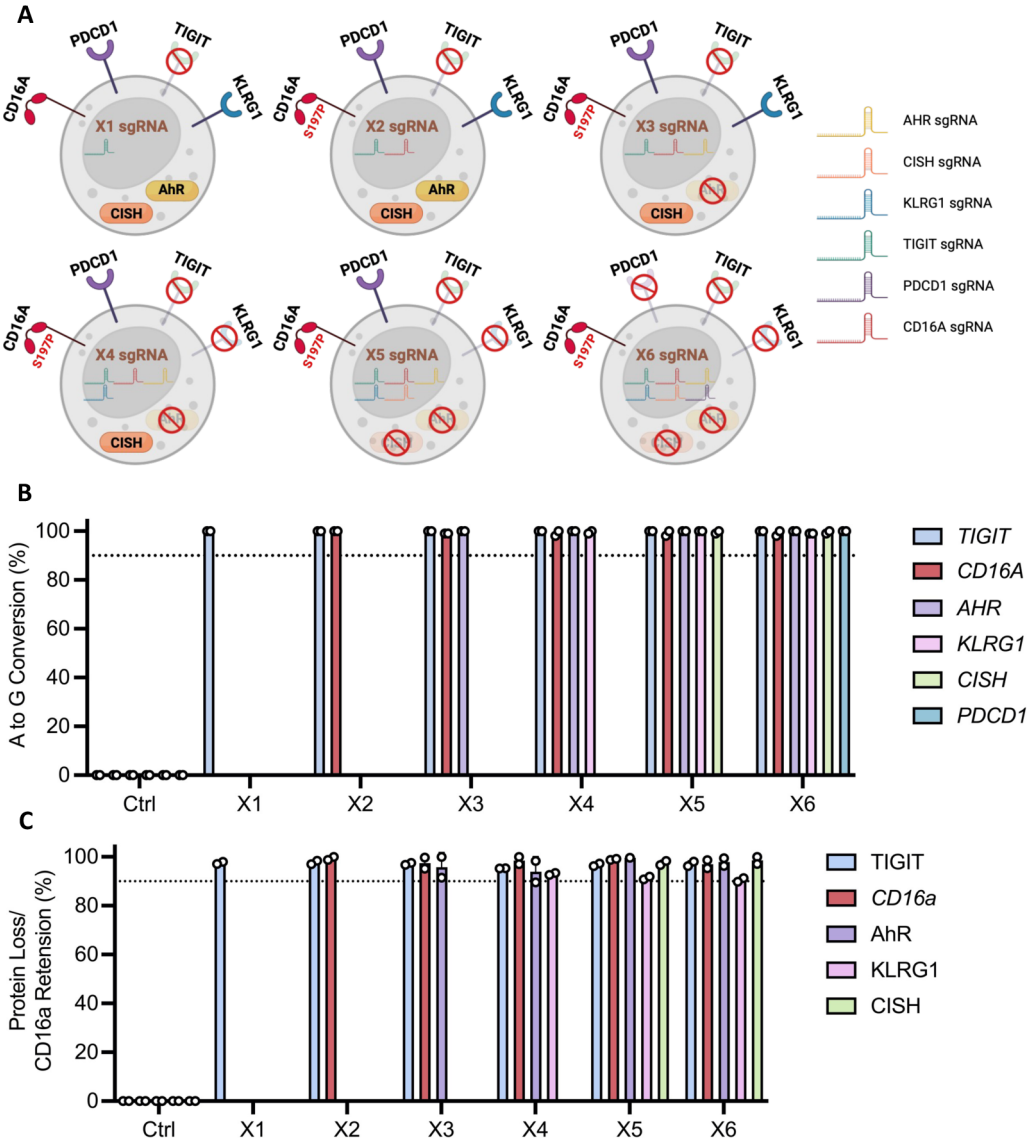

Figure 3 Highly efficient multiplex editing in NK cells using BE. (A) Schema of multiplex editing strategy. (B) Multiplex editing efficiency at genomic level quantified by A-to-G conversion of target base for each gene locus (n=2 independent NK cell donors). (C) Multiplex editing efficiency at protein level quantified by percentage of protein loss of each gene (n=2 independent NK cell donors). Data represented as mean±SD. AHR, Aryl hydrocarbon receptor; BE, base editor; CISH, cytokine-inducible SH2-containing protein; KLRG1, killer cell lectin-like receptor subfamily G member 1; NK, natural killer; PDCD1, programmed cell death protein 1; sgRNA, guide RNA; TIGIT, T cell immunoreceptor with Ig and ITIM domains.

cell function.[28] Here, we examined whether the same approach can be applied in developing NK-based cell therapies using ABE8e and also attempted to find the upper limits of multiplex base editing. We started with one sgRNA targeting *TIGIT* and subsequently added sgRNAs one at a time in the following order: ncCD16a sgRNA, AHR sgRNA, KLRG1 sgRNA, CISH sgRNA, PDCD1 sgRNA up to a total of six sgRNAs (figure 3A). Multiplex editing efficiencies at the genomic level were again assessed via Sanger sequencing of A-to-G conversions at target sites assessed using EditR. Impressively, we observed no significant loss of editing efficiency at any loci using up to six sgRNAs simultaneously (figure 3B and online supplemental figure 6A–F). To evaluate the potential off-target effect of multiplex base editing, the top 8–10 computationally predicted off-target sites of each gRNA were examined through rhAmpSeq analysis, which identified no detectable off-target editing at any site (online supplemental figure 6G). The only one exception is for PDCD1 sgRNA, however, the detected off-target site is in a non-coding region (online supplemental figure 6G). Editing efficiencies at the protein level, measured by protein loss (for AhR, CISH, KLRG1, TIGIT, and PD-1) or CD16a retention rate after PMA treatment were consistent with genomic base editing levels (figure 3C and online supplemental figure 7A–E). In summary, these data demonstrate that highly efficient multiplex base editing is achievable in NK cells using ABE and the upper limit of simultaneous base edits

without compromising editing efficiencies has not yet been reached in this context.

Tailored multiplex engineering of NK cells for optimized cytotoxicity against Raji CD155^{hi}/PD-L1^{hi} cells

In order to demonstrate a tailored editing approach for NK-based cancer immunotherapy, we next sought to determine an optimal combination of multiplex edits that yields the most potent NK cell cytotoxicity for a chosen tumor model. Two of the most common factors associated with poor prognosis in many cancers are high expression of PD-L1 and CD155.[68–76] To model this, we generated a Raji cell line that overexpresses both checkpoint ligands (ie, Raji$^{hi/hi}$) (online supplemental figure 8). To determine the optimal multiplex base editing combination, we started with TIGIT (CD155 ligand) and PDCD1 (PD-L1 ligand) KO to avoid suppression from CD155 and PD1, respectively. Next, these edits were combined with AHR KO, CISH KO, or both KOs for testing different base editing combinations (figure 4A). Editing efficiencies showed the average A-to-G conversions of each target site in all combinations were above 90%, and similar results were observed for average protein loss of all KOs (figure 4B,C). In order to assess the functional consequences of the various combinations of base edits, we first performed co-culture killing assays with Raji$^{hi/hi}$ cells at different E:T ratios. We observed that unedited NK cells had the lowest level of killing against Raji$^{hi/hi}$ and there was no significant difference in killing between TIGIT+PDCD1 (TP) KO NK, TIGIT+PDCD1+AHR (TPA) KO NK, and TIGIT+PDCD1+AHR+CISH (TPAC) KO NK. However, knocking out TIGIT, PDCD1, and CISH (TPC) demonstrated the highest killing against Raji$^{hi/hi}$ cells compared with all other combinations (figure 4D,E and online supplemental figure 9A–D). These data demonstrate that TPC KO NK cells have the most robust cytotoxicity against Raji$^{hi/hi}$ cells compared with all other multiplex base editing combinations.

Simultaneous multiplex base editing and non-viral transposon engineering generate highly functional CAR-NK cells

To date, delivery of CAR constructs into NK cells has been largely limited to the use of viral vectors.[77–79] The cost and extended manufacturing process of viral vectors drive the need for a faster and more economical alternative method for stable transgene delivery. Thus, to develop an effective non-viral engineered CAR-NK cell product, we designed a *TcBuster* transposon plasmid encoding a CD19 CAR (figure 5A; "CAR"). In an effort to test whether cytokine armoring of CAR-NKs would enhance persistence and activity, we designed an additional transposon plasmid encoding sIL15 (figure 5A; "CAR15"). Notably, IL15 has been shown to be necessary to support NK cell persistence in NOD-scid IL2R gamma-null (NSG) models.[80 81] Each transposon contains the MND promoter, second generation CD19-targeting CAR, and RQR8 (figure 5A). RQR8 is a synthetic cell surface receptor with CD34 and CD20 epitopes and was included here for flow cytometry detection and immunomagnetic enrichment of CAR-expressing NK cells.[82]

For engineering, NK cells were feeder expanded before codelivery of CD19 CAR transposon plasmid, *TcBuster* transposase mRNA, sgRNAs, and ABE8e mRNA through electroporation (figure 5B). Following a subsequent 7-day NK cell feeder expansion, the CD19 CAR integration rate was assessed via flow cytometry before CAR enrichment through RQR8 immunomagnetic selection (figure 5C). CAR integration rates in each group were reasonably efficient in multiple donors (57.4–81.3% for CAR and 20.1–39.9% for CAR15) and comparable to previously reported integration rates of CD19 CAR through retroviral transduction.[77 79] Transposon copy number analysis of CAR or CAR15 NK cells indicated a relatively consistent copy number among all CAR-expressing groups (online supplemental figure 10A). Since transposon systems exhibit a semirandom integration pattern, we also assessed the insertion site profile of *TcBuster* transposons and found that it integrated in and near coding genes less frequently than lentivirus or retrovirus regardless of construct (online supplemental figure 10B). Additionally, evaluation of the distance between integration events and transcriptional start sites indicated that *TcBuster* integrated further away from transcriptional start sites when compared with lentivirus and retrovirus (online supplemental figure 10C). CAR enrichment was further performed to ensure CAR expression across groups was not significantly different, which could confound results comparing across groups. After a third and final feeder-based expansion, CD19 CAR expression was assessed by flow cytometry (figure 5C) and IL-15 expression was confirmed through ELISA (online supplemental figure 11; CAR15: 220.0±5.09 pg/mL, CAR15/TPC^{KO}: 340.9±20.34 pg/mL). Control groups lacking transposon engineering demonstrated base editing levels comparable to previous results in TPC KO NK cells (figure 4B), while a 10–25% reduction in base editing efficiency was observed in groups with transposon codelivery (figure 5D). However, the average protein reduction of each gene of interest in all KO groups was above 90%, with one outlier NK donor from the CAR15/TPC^{KO} group having lower TIGIT protein reduction (figure 5E). To examine whether multiplex base editing in NK cells results in any detectable chromosomal translocations, we designed a droplet digital PCR (ddPCR) assay to examine both 5' and 3' translocations of all KO genes targeted (*CISH*, *TIGIT*, and *PDCD1*) (online supplemental figure 10D). Using Cas9 nuclease combined with all three gRNAs as a positive control for maximum translocations, we found undetectable levels of chromosomal translocations occurring in multiplex base-edited NK cells, with or without simultaneous CD19 CAR integration (online supplemental figure 10E).

The functionality of all engineered NK cell groups was first assessed using co-culture killing assays with Raji$^{hi/hi}$ cells at a range of E:T ratios. We observed no significant differences in killing between CAR and CAR15 groups, but a moderate enhancement of killing by the CAR15/TPC^{KO} group compared with CAR/TPC^{KO} NK cells (figure 5F,G and online supplemental figure 12A–D). TPC^{KO} also improved cytotoxicity of NK cells, with both CAR/TPC^{KO} and CAR15/TPC^{KO} groups exhibiting better killing against Raji$^{hi/hi}$ cells when compared with that of their corresponding CD19 CAR

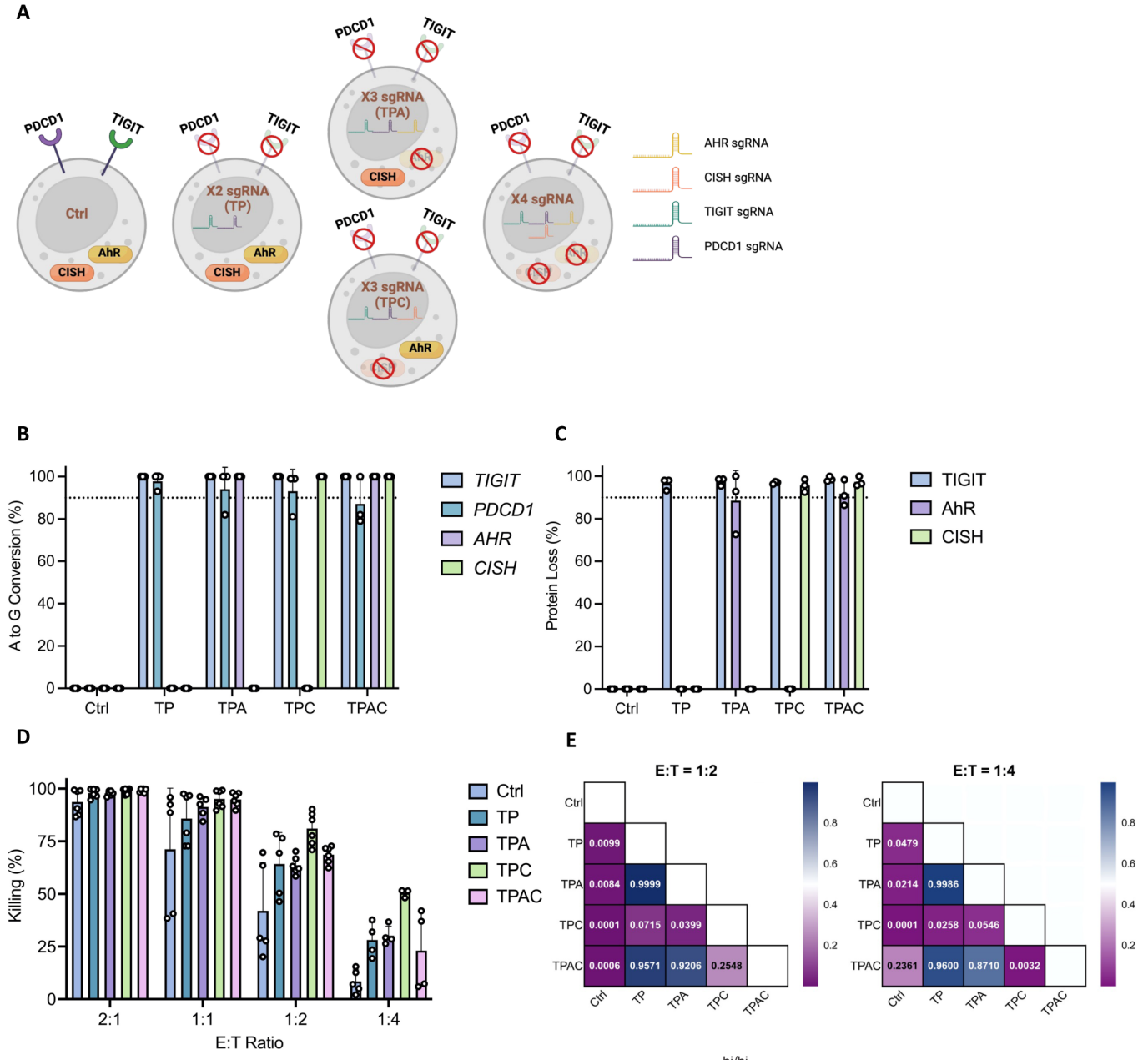

Figure 4 Optimization of multiplex KO to maximize NK functionality against Raji$^{hi/hi}$. (A) Schema of optimization strategy and all possible KO combinations included. (B) Editing efficiency at genomic level quantified by A-to-G conversion of target base for each gene locus (n=3 independent NK cell donors). (C) Editing efficiency at protein level quantified by percentage of protein loss of each gene (n=3 independent NK cell donors). (D) Ability of each KO combination to kill Raji$^{hi/hi}$ cells at various E:T ratios as measured by luciferase luminescence assay. Assays run in triplicate in n=2 independent biological NK cell donors. (E) Functional killing assay statistical significance (p value) between each KO combination at E to T ratio of 1:2 and 1:4. Data represented as mean±SD. P values calculated by two-way ANOVA test. ANOVA, analysis of variance; AHR, Aryl hydrocarbon receptor; CISH, cytokine-inducible SH2-containing protein; Ctrl, ABE8e mRNA only; E:T, effector-to-target; KO, knockout; mRNA, messenger RNA; NK, natural killer; PDCD1, programmed cell death protein 1; sgRNA, guide RNA; TIGIT, T cell immunoreceptor with Ig and ITIM domains; TP, *TIGIT* and *PDCD1* KO; TPA, *TIGIT*, *PDCD1*, and *AHR* KO; TPAC, *TIGIT*, *PDCD1*, *AHR,* and *CISH* KO; TPC, *TIGIT*, *PDCD1*, and *CISH* KO.

only groups. These data demonstrate that CAR15/TPC^{KO} NK cells exhibited the most significant functionality improvement against Raji$^{hi/hi}$ targets in vitro.

Multiplex base-edited CD19 CAR-NK cells are highly functional in vivo

To test the efficacy of our multiplex base-edited CAR-NK cell product in vivo, we used Raji$^{hi/hi}$ cells as a highly suppressive xenograft model of Burkitt's lymphoma. NSG mice were xenografted with 1E5 of Raji$^{hi/hi}$ through intravenous injection on day 0, followed by a randomization

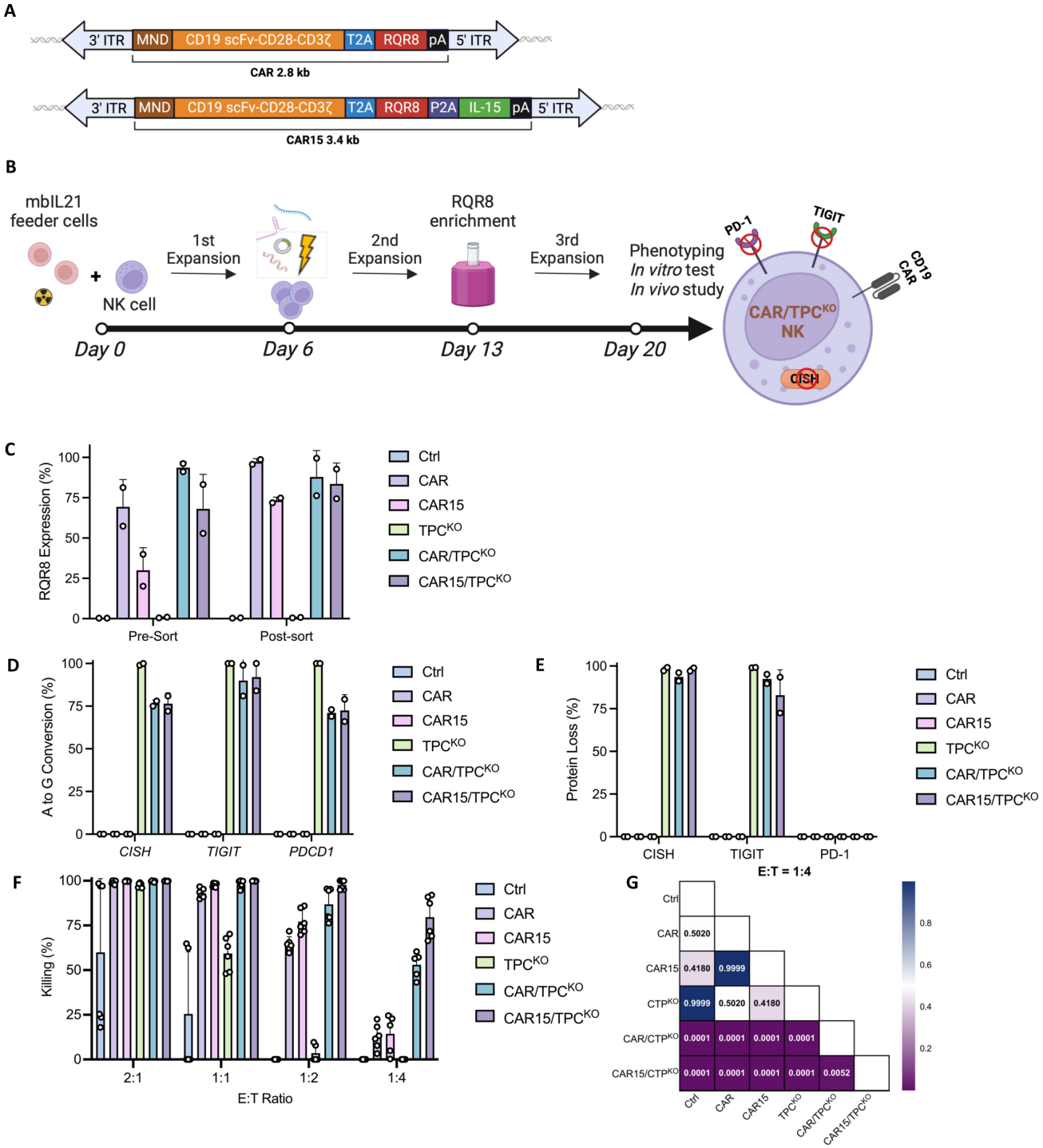

Figure 5 Simultaneous BE and non-viral transposon engineering exhibited enhanced NK cytotoxicity. (A) Schema of the designs of CD19 CAR constructs. (B) Schema of NK cell engineering timeline for simultaneous sgRNAs and CD19 CAR delivery. (C) Presorting and postsorting CAR integration rate quantified by percentage of RQR8 expression on NK cells (n=2 independent NK cell donors). (D) Postsorting editing efficiency at genomic level quantified by A-to-G conversion of target base for each gene locus (n=2 independent NK cell donors). (E) Postsorting editing efficiency at protein level quantified by percentage of protein loss of each gene (n=2 independent NK cell donors). (F) *In vitro* testing of the cytotoxicity of simultaneous BE and *TcBuster* engineered NK cells against Raji$^{hi/hi}$ cells at various E:T ratios as measured by luciferase luminescence assay. Assays run in triplicate in n=2 independent biological NK cell donors. (G) Killing assay statistical significance (p value) between each condition at E to T ratio of 1:4. Data represented as mean±SD. P values calculated by two-way ANOVA test. ANOVA, analysis of variance; BE, base editor; CAR, CD19 CAR RQR8; CAR15, CD19 CAR RQR8 IL-15; CAR/CTP^{KO}, CD19 CAR RQR8 with *CISH*, *TIGIT*, and *PDCD1* KO; CAR15/CTP^{KO}, CD19 CAR RQR8 IL-15 with *CISH*, *TIGIT*, and *PDCD1* KO; CISH, cytokine-inducible SH2-containing protein; Ctrl, ABE8e mRNA and CAR-expressing nanoplasmid only; CTP^{KO}, *CISH*, *TIGIT*, and *PDCD1* KO; E:T, effector-to-target; KO, knockout; NK, natural killer; PDCD1, programmed cell death protein 1; sgRNA, guide RNA; TIGIT, T cell immunoreceptor with Ig and ITIM domains; TPC, *TIGIT*, *PDCD1*, and *CISH* KO.

into treatment groups of equivalent tumor burden prior to therapy delivery (online supplemental figure 13A). Mice receiving therapy were dosed with two rounds of engineered NK cells 14 days apart (day 3 and 17) (figure 6A). Mouse body weight and bioluminescent imaging (BLI) of tumor burden were monitored weekly until predefined humane endpoints were reached (figure 6B and online supplemental figure 13B). BLI results suggested tumor progression was significantly delayed in groups treated with CAR15 NK (n=5) and CAR15/TPC^{KO} NK (n=5) compared with all other groups (figure 6B). Mouse tumor burden of these two groups was significantly reduced by day 23, the last imaging time point before mice began to meet endpoint criteria (figure 6C). The survival of mice receiving CAR15 and CAR15/TPC^{KO} NK was significantly improved compared with control NK treated animals (figure 6D median survival in days: CAR15 vs Ctrl, 63 vs 25, p<0.01; CAR15/TPC^{KO} vs Ctrl, 30 vs 25, p<0.05).

Next, we took a closer look at the animals receiving CAR15 or CAR15/TPC^{KO} treatment. Among all five mice in the CAR15 group, four animals were found with tumor burden in bone marrow (BM) and spleen and one animal had tumor burden only in a potentially immune-privileged area (ovary) (figure 6E). For the CAR15/TPC^{KO} group, one animal was found with tumor burden in BM and spleen, one animal had tumor burden only in potentially immune-privileged areas (ovary and brain), and three animals with unexplained systemic toxicity had minimum residual disease (figure 6E). Histology of ovary and brain tumors indicated a dominance of hCD19+cells with no signs of hCD56+NK cells (online supplemental figure 13D). After excluding animals with tumors in seemingly immune-privileged areas in CAR15 and CAR15/TPC^{KO} groups, we observed significantly higher endpoint tumor burden in mice from the CAR15 group when compared with that of CAR15/TPC^{KO} groups (figure 6F).

Additionally, weekly PB collection and endpoint PB, BM and spleen collections were performed to monitor the expansion and persistence of NK cells in each treatment group (figure 6G, online supplemental figure 13E). We observed a significantly higher level of NK cells in PB, BM and spleen at endpoint in the CAR15/TPC^{KO} NK group than in any other groups (figure 6G). Interestingly, the CAR15 group had minimum detectable NK cells in PB and no NK cells in the BM or spleen (figure 6G). Moreover, weekly monitoring of NK cells in PB identified a significantly more rapid expansion of NK cells in mice from the CAR15/TPC^{KO} group than from the CAR15 group in a short time span (day 25 to day 30), shortly before the suspected systemic toxicity was observed in mice from the CAR15/TPC^{KO} group (figure 6H).

With the stochastic systemic toxicity greatly compromising the significance of the *in vivo* validation of our NK cell product, we decided to re-run *in vivo* studies with CAR15 integration groups to increase the power of this study. The tumor model and experimental design were identical to figure 6A. Similar to the previous study, BLI indicated a significantly delayed tumor progression of CAR15 and CAR15/TPC^{KO} groups compared with phosphate-buffered saline (PBS) and control groups (figure 7A). More importantly, the CAR15/TPC^{KO} group exhibited slower tumor progression than the CAR15 counterpart, with four mice showing tumor burden well under control at the end of the study (figure 7A). By day 23, the last imaging time point before control mice began to meet endpoint criteria, tumor burden of CAR15 and CAR15/TPC^{KO} groups was significantly reduced when compared with control NK (figure 7B). The survival of mice receiving CAR15 and CAR15/TPC^{KO} NK was, again, significantly longer than control groups (figure 7C). The median survival of the CAR15/TPC^{KO} group was longer than CAR15 as well (figure 7C) (95.5 vs 54.5 days). However, three mice in CAR15/TPC^{KO} again died of systemic toxicity.

Using a similar strategy as the previous *in vivo* study, we further stratified mice in CAR15 and CAR15/TPC^{KO} groups by cause of death (or with tumor fully controlled by the end of the study), as shown in figure 7D. After excluding mice with tumors in a potentially immune-privileged area, the average tumor burden at termination is significantly lower in the CAR15/TPC^{KO} group than in the CAR15 group (figure 7E). In summary, we observed a significant improvement in tumor control and overall survival of mice treated with NK cells expressing sIL-15, with the CAR15/TPC^{KO} NK group exhibiting significantly better tumor control and a slightly better overall survival when compared with CAR15 NK treated animals.

DISCUSSION

Cellular therapy using CAR-expressing primary effector cells has shown great success in the clinic and resulted in multiple Food and Drug Administration (FDA)-approved treatments for hematologic malignancies and solid tumors.[2] These current-generation FDA-approved CAR therapies largely use autologous α/β T cell chassis and viral vector engineering methods, which limits the scope of potential therapy recipients and results in high manufacturing costs and long timelines. A more appealing approach is to use a universal cell type, such as primary NK cells, that are engineered using non-viral methods. Further, as the landscape of cancer therapy shifts towards solid tumors, it is increasingly evident that methods such as cytokine armoring and immune checkpoint editing through genome engineering will be required to create more potent and persistent therapies. Since CRISPR/Cas9 was co-opted for genome editing over a decade ago, engineering efficiencies in primary immune cells have been significantly improved.[83 84] It remains, however, that insertions or deletions (indels) and translocations caused by Cas9-induced DSBs could negatively impact cellular function and introduce major safety concerns for CRISPR/Cas9-based therapies.[83 85] In an effort to circumvent this issue, we applied base editing technology to NK cell engineering for the first time and demonstrated NK cells could be multiplex engineered with undetectable rates of indels. KO of our selected targets or installation of gain-of-function edits resulted in increased baseline functionality, which could be combined to further increase performance. We then combined multiplex base

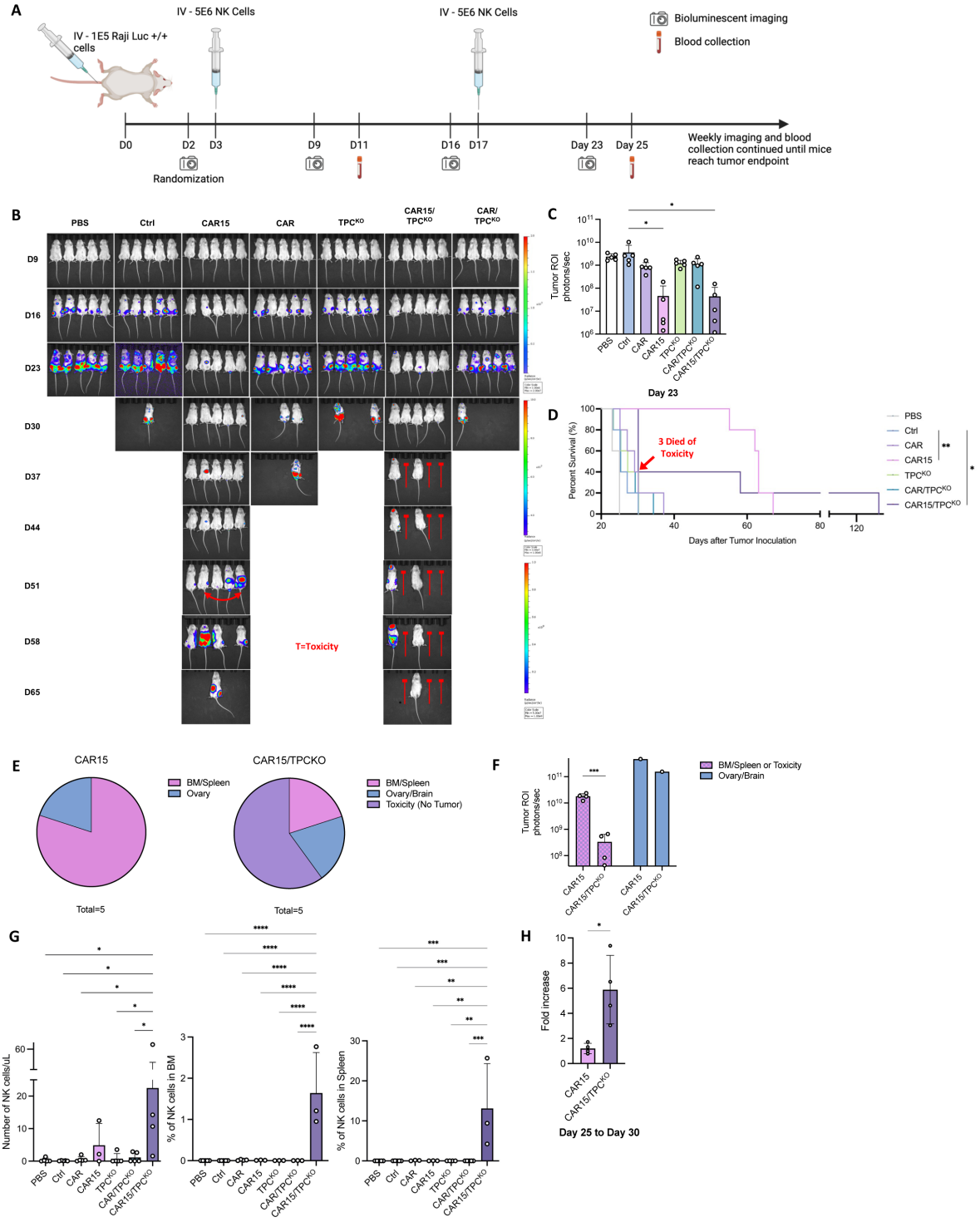

Figure 6 Multiplex edited CD19 CAR-NK cells are highly functional in vivo. (A) Schema of in vivo study design and timeline. (B) Luminescence (ROI) of individual tumor burden of mice bearing Raji$^{hi/hi}$ cells following treatment with PBS, Ctrl or engineered NK cells. Toxicity: mouse died due to suspected systemic toxicity, that is, rapid weight loss (>20%). (C) Tumor burden of each group on day 23, quantified by ROI (photons/sec) of each mouse (n=5). (D) Survival curve of each group shown in Kaplan-Meier curve (n=5). P values calculated by the Mantel-Cox test. Ctrl versus CAR15, **p≤0.01; Ctrl versus CAR15/CTP^{KO}, *p≤0.05. (E) Cause of death of each animal in CAR15 and CAR15/CTP^{KO} groups (n=5). BM/spleen: tumor ROI ≥ 1E8 with no obvious ovary and/or brain tumor; Ovary/brain: tumor ROI ≥ 1E8 with obvious ovary and/or brain tumor; Toxicity (No tumor): tumor ROI < 1E8. (F) Tumor burden of CAR15 and CAR15/CTP^{KO} group at endpoint stratified by cause of death. (G) Quantifications of the number of NK cells in peripheral blood (measured by NK cell number per µL of blood), BM and spleen (measured by percentage of NK cells in BM or spleen) at end point. (H) Quantification of NK cell expansion in CAR15 and CAR15/TPC^{KO} groups between day 25 and 30 (fold increase: day 30 NK cell count vs day 25 NK cell count). P values calculated by one-way ANOVA test (*p≤0.05, **p≤0.01, ***p≤0.001, ****p≤0.0001). Data represented as mean±SD. ANOVA, analysis of variance; BM, bone marrow; CAR, chimeric antigen receptor; IV, intravenous; NK, natural killer; PBS, phosphate-buffered saline.

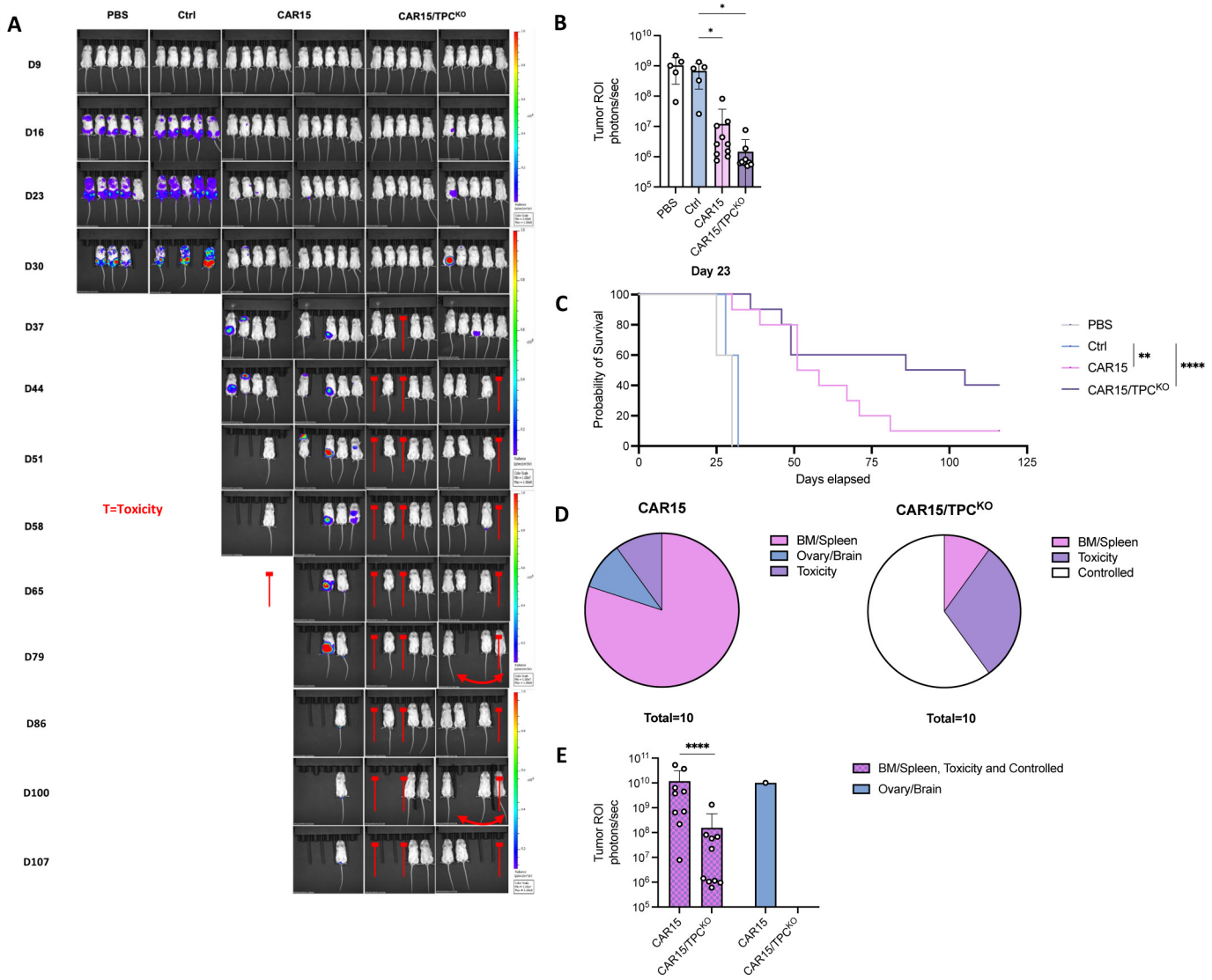

Figure 7 Large-scale *in vivo* study of CAR15 and CAR15/CTP^{KO} NK cells. (A) Luminescence (ROI) of individual tumor burden of mice bearing Raji$^{hi/hi}$ cells following treatment with PBS, Control or engineered NK cells. Toxicity: mouse died due to suspected systemic toxicity, that is, rapid weight loss (>20%) with less than 75 days of survival. (B) Tumor burden of each group on day 23, quantified by ROI (photons/sec) of each mouse (n=5). (C) Survival curve of each group shown in Kaplan-Meier curve (PBS and Ctrl, n=5; CAR15 and CAR15/CTP^{KO}, n=10). P values calculated by Mantel-Cox test. Ctrl versus CAR15, **p≤0.01; Ctrl versus CAR15/CTP^{KO}, ****p≤0.001. (D) Cause of death of each animal in CAR15 and CAR15/CTP^{KO} groups (n=10) is defined based on the following criteria. BM/Spleen: tumor ROI ≥ 1E8 with no obvious ovary and/or brain tumor; Ovary/brain: tumor ROI ≥ 1E8 with obvious ovary and/or brain tumor; Toxicity (No tumor): tumor ROI < 1E8 w/ < 75 days of survival; Cleared: tumor ROI <1E8 and ≥75 days of survival. (E) Tumor burden of CAR15 and CAR15/CTP^{KO} groups at endpoint stratified by cause of death. P values calculated by one-way ANOVA test (*p≤0.05, **p≤0.01, ****p≤0.0001). Data represented as mean±SD. ANOVA, analysis of variance; BM, bone marrow; CAR, chimeric antigen receptor; NK, natural killer; PBS, phosphate-buffered saline.

editing with non-viral transposon engineering to generate a CAR-NK engineering pipeline for precision enhancement of next-generation CAR-NK cell products. These multiplex base-edited CAR-NK cells showed improved functionality *in vitro* and *in vivo* against a challenging model of Burkitt's lymphoma and provide compelling preclinical evidence for a future NK-based CAR therapy option.

Our initial engineering studies examined whether NK cells were amenable to individual targeted base editing at high frequency and how these edits impact NK cell function. We began with selecting a variety of targets that play inhibitory but critical roles in NK cell function with an emphasis on clinical relevance. To confirm that successful genetic modifications lead to protein loss and functional enhancements, we validated protein loss and functional improvement as part of the validation process, respectively. Other than *KLRG1*, all inhibitory target KOs exhibited the predicted functional enhancement. *KLRG1* KO NK cells' failure to demonstrate improved function is in line with some previous studies disrupting *KLRG1* in NK cells.[86] As speculated in those studies, this contradictory finding may be attributed to a relatively low inhibitory potential of *KLRG1* on NK cell function.[86 87] Additional testing in a more relevant cell line model may

be required to better understand the role of KLRG1 in NK cell functionality.

Our inability to detect PD-1 protein on the surface of NK cells is in line with numerous previous reports and reflects the ongoing controversy of the role of PD-1 in NK cells.[23 53 88 89] For instance, the Moretta group has published multiple studies on this issue and found that NK cells constantly produce PD-1 mRNA and protein, but only rapidly externalize PD-1 protein on activation by certain stimuli.[88] Davis *et al* also reported minimal surface expression of PD-1 in NK cells from healthy individuals.[89] Moreover, several previous studies have used functional assays with anti-PD-1 agents to validate PD-1 expression on the NK cell surface, and our results here demonstrating significant cytotoxicity improvement of *PDCD1* KO NK cells against *PD-L1*+ target cells further support the role of PDCD1 in NK cell inhibition by PD-L1.[23 53]

We also demonstrate the ability to install gain-of-function mutations in NK cells using base editing. The rapid downregulation of CD16a as a result of a proteolytic cleavage process on NK cell activation serves as a negative feedback mechanism for ADCC. In a TME setting, functional inactivation of tumor-associated NK cells reflects a further down-regulation of CD16a that significantly compromises NK cell cytolytic function against tumor cells.[90 91] BE installation of ncCD16a improved both ADCC-mediated killing and cytokine production in NK cells. Notably, this BE-mediated approach is likely significantly safer and more physiologically relevant compared with integration of a ncCD16A cDNA expression cassette using viral delivery.[67] Unexpectedly, we also observed a significant improvement in basal killing of Raji cells with ncCD16A NK cells. We speculate that the constitutive expression of ncCD16a may result in low-level tonic signaling, contributing to this phenomenon. This phenomenon could further benefit patients with compromised NK cytolytic functions, and a closer look at the downstream mechanisms of this phenomenon is warranted in future studies.

Moving forward to multiplex editing, we observed no significant reduction of editing efficiencies with up to six codelivered sgRNAs. Surprisingly, there was an improvement in *KLRG1* KO efficiency at the multiplex level compared with the single-target experiments. One explanation for this phenomenon is a potential "carrier effect" linked to increasing the total amount of codelivered sgRNAs. This is similar to previous studies reporting that a higher extracellular DNA concentration leads to a higher amount of DNA delivered to the nucleus.[92 93] However, further investigation is required to illuminate the exact mechanisms behind this observation.

To examine whether multiplex editing resulted in enhanced *in vitro* function, we developed and used an engineered Burkitt's lymphoma cell line Raji$^{hi/hi}$ as a proof-of-principle model. We hypothesized that the number of inhibitory gene KOs would positively correlate with the improvement of NK cell function, and selected *AHR*, *CISH*, *TIGIT* and *PDCD1* as candidates. *KLRG1* was excluded due to its failure to demonstrate functional improvement at single KO level. Contrary to our hypothesis, the TPC KO group demonstrated the most significant improvement in cytotoxicity against Raji$^{hi/hi}$ cells. Additionally, the fact that no significant differences in killing were observed among TP, TPA, and TPAC KO groups throughout all E:T ratios is another interesting finding that warrants further investigation. It is possible that Raji$^{hi/hi}$ cells produced lower amounts of AhR ligand (kynurenine) than K562, leading to a less pronounced inhibitory effect on NK cells. These findings suggest that the number of inhibitory gene KOs does not always correlate with improved NK cell functionality, and an optimization of the KO combination is likely required for precision enhancement against each unique tumor type of interest.

Finally, in an effort to test the impacts of multiplex editing on CAR-NK cell function, we codelivered a CD19 CAR with multiplex base editing using the *TcBuster* DNA transposon system. Compared with traditional virus-based delivery methods, non-viral transposon systems significantly reduce the manufacturing cost and timelines, with a capacity for large genetic cargo delivery. Integration efficiencies of CD19 CAR constructs were correlated with its cargo size, and are comparable to that of virus-based delivery methods.[22 94] One unexpected finding is the significantly higher CD19 CAR integration rate in the groups with TPC KO. We suspect a similar carrier effect may be contributing to the higher rates; however, further investigation is necessary to define the mechanism behind this observation.[92 93] We also examined the transposon copy number of each CAR-NK product as copy number is a critical parameter for clinical translation. A 2021 clinical trial using the *PiggyBac* transposon to generate CAR-T cells for relapsed and refractory CD19+malignancy reported that 2 out of 10 patients developed CAR-T lymphoma following treatment. Further investigation into these cases revealed significantly higher transgene copy numbers (24–29.8 copies per cell) in both the CAR-T product in PB and the resulting malignancy, underscoring the importance of controlling copy number in transposon-engineered cell products.[95 96] All of our CAR-NK products have copy numbers below 10, which is within the range that has been deemed safe and acceptable for advancing to evaluation in clinical trials.[97] Multiple previous studies have reported improved *in vivo* persistence of CAR-NK cells with sIL-15 expression.[20–22 98] Here, we adopted this idea in an attempt to improve proliferation and prolong the persistence of NK cell products *in vivo* by armoring cells with sIL-15. Our animal study clearly demonstrated a strong correlation of IL-15 expression with NK cell persistence *in vivo*, which translates into a significantly delayed tumor progression and improved overall survival compared with groups without IL-15 expression. For groups treated with NK cells expressing sIL-15, one animal from group CAR15 developed a tumor in the ovary, and two animals from group CAR15/TPC^{KO} developed a tumor in the ovary and/or brain. The fact that all these tumors developed in known immune-privileged areas serves as indirect evidence of

robust tumor clearance in PB and BM where full immune surveillance is expected.[99]

Although CAR15/TPC^{KO} treated mice demonstrated significantly delayed tumor progression compared with CAR15 treated mice, its failure to exhibit improved survival over CAR15 is unexpected based on our *in vitro* results and thus requires closer examination. In the initial animal study, among all five animals in the CAR15/TPC^{KO} group, three died of suspected systemic toxicity with relatively low tumor burden but met endpoint criteria of significant decrease of body weight. We initially suspected cytokine release syndrome (CRS) in these mice; however, there was no significant increase in CRS-related cytokines in serum at the endpoint (data not shown). Our observation is consistent with a previous study using sIL-15 expressing CAR-NK cells, which also found negative evidence of CRS and attributed the observed systemic toxicity to rapid NK cell expansion *in vivo*.[98] A closer look at the weekly and endpoint NK cell numbers in PB revealed a rapid NK cell expansion after day 25 in four out of five mice in the CAR15/TPC^{KO} group, and three of those mice died in the following week due to suspected systemic toxicity (figure 6G and online supplemental figure 13E). It is also worth noting that in the follow-up *in vivo* study we observed systemic toxicity in 3/10 mice from the CAR15/TPC^{KO} group and 1/10 mice in the CAR15 group. These observations suggested a potential mouse model compatibility issue that is worth additional investigation that is beyond the scope of this study. While further investigations of the suspected systemic toxicity in the CAR15/TPC^{KO} group are warranted, it is accurate to conclude that CAR15/TPC^{KO} NK treatment is significantly more efficient at delaying tumor progression over CAR15 NK, with a trend toward further benefit in survival over CAR15 as well.

In summary, we reported the first application of BE in primary NK cells, with high editing efficiency for both single and multiplex editing. Moreover, with codelivery of a multi-cistronic CAR construct using a non-viral transposon system, we present a highly flexible, fully non-viral engineering platform that allows precision enhancement of NK-based cell therapy against various types of cancer. With our proof-of-principle model, we have generated a pipeline for developing a highly customized NK product for any specific type of cancer. Moving forward, we are actively exploring the application of this platform into the frontier of solid tumors, including enhancement of NK cell homing to tumor sites, NK cell resistance to oxidative stress, and more.

MATERIALS AND METHODS

Production of editing reagents

ABE8e plasmid was obtained from Addgene (https://www.addgene.org/138489/) and cloned into a pmRNA vector. ABE8e mRNA was produced by Trilink BioTechnologies. The mRNA transcript is modified with full substitution of Pseudo-U and 5-Methyl-C, and capped using CleanCap AG. Nanoplasmids for CD19 CAR were synthesized by Aldevron.

Guide RNA design

sgRNAs for KO were designed using the base editing splice-site disruption sgRNA design program SpliceR (https://z.umn.edu/splicer). SpliceR is written in the R statistical programming language (V.3.4.3). Briefly, SpliceR takes a target Ensembl transcript ID, a BE PAM variant, and a species as input. Using the exon and intron sequences from Ensembl, the program extracts the region surrounding every splice site based on a user-specified window. The pattern of N20-NGG is then matched to the antisense strand of the extracted sequence. Matched patterns are then scored based on the position of the target motif within the predicted editing window based on previous publications. Subsequently, sgRNAs are scored based on their position within the transcript, where sgRNAs earlier in the transcript receive a higher score. sgRNA for ncCD16a was designed manually to achieve the S197P mutation.

Donor NK cell isolation

Peripheral blood mononuclear cells (PBMCs) from healthy human donors were obtained by automated leukapheresis (Memorial Blood Centers, Minneapolis, Minnesota, USA). CD56+CD3 NK cells were isolated from the PBMC population using the EasySep Human NK Cell Isolation Kit (STEMCELL Technologies, Cambridge, Massachusetts, USA). NK cells were frozen at 2.5E6 or 5E6 cells/mL in CryoStor CS10 (STEMCELL Technologies, Cambridge, Massachusetts, USA).

NK cell culture

NK cells were cultured in CTS AIM V (Thermo Fisher, Waltham, Massachusetts, USA) with 5% CTS Immune cell SR (Thermo Fisher, Waltham, Massachusetts, USA), and 100 IU/mL IL-2 (PeproTech, Rocky Hill, New Jersey, USA). NK cells were activated by co-culture with X-irradiated (100 Gray) feeder cells (K562 expressing membrane-bound IL-21 and 41BB-L) at various feeder to NK ratios (2:1 prior to electroporation, 5:1 72 hours after Neon electroporation, or 1:1 immediately after MaxCyte electroporation).

NK cell electroporation

Neon electroporation

Feeder cell-activated NK cells were washed once with PBS (Ca^{2+} and Mg^{2+} free) and resuspended at 3E7 cells/mL in electroporation buffer. Protector RNase inhibitor (Sigma-Aldrich, St Louis, Missouri, USA) was added to the mixture at a concentration of 0.8 U/µL and incubated for 5 min at room temperature. The cell mixture was added to 1.5 µg of ABE8e mRNA and 1 nmol sgRNA on ice. This mixture was electroporated in a 10 µL tip using the Neon Transfection System (Thermo Fisher, Waltham, Massachusetts, USA) under the following conditions: 1825 volts, pulse width of 10 ms, 2 pulses. NK cells were allowed to recover at a density of 1E6 cells/mL in antibiotic-free medium containing 100 IU/mL IL-2 (PeproTech, Rocky Hill, New Jersey, USA) for 72 hours at 37°C, before expansion with feeder cells at a 5:1 feeder to

NK ratio. Single and multiplex base editing of NK cells was engineered using this platform.

MaxCyte electroporation

NK cells reaching a 10-fold increase in cell number after feeder cell expansion were washed once with electroporation buffer and resuspended at 1.75E8-1.00E9 cells/mL. Protector RNase inhibitor (Sigma-Aldrich, St Louis, Missouri, USA) was added to the mixture at a concentration of 0.8 U/µL and incubated for 5 min at room temperature. The cell mixture was added to 4 ug of ABE8e mRNA, 5 µg sgRNA, 3 µg of transposase mRNA and 5 µg transposon nanoplasmid on ice. This mixture was electroporated in an R-50×3 assembly using the MaxCyte System (Thermo Fisher, Waltham, Massachusetts, USA) under Expanded T Cell 4 protocol. NK cells were allowed to recover at a density of 1E6 cells/mL in antibiotic-free medium for 1 hour at 37°C, before expansion with feeder cells at a 1:1 feeder to NK ratio. *TcBuster* transposon integration in combination with multiplex base editing of NK cells was engineered using this platform.

Genomic DNA analysis

NK cells were harvested 10 days after electroporation, followed by DNA isolation and PCR amplification of CRISPR-targeted loci using Phire Tissue Direct PCR Master Mix kit (Thermo Fisher, Waltham, Massachusetts, USA). Base editing efficiency was analyzed at the genomic level by Sanger sequencing of the PCR amplicons, and subsequent analysis of the Sanger sequencing traces using the web app EditR (baseeditr.com).[44]

Primer and sequence

Primer name	Primer sequence
AHR Exon 2 Splice Donor forward	TAC CAT GCA TCA TTT CAG TG
AHR Exon 2 Splice Donor reverse	TTT CAG AGT AAA GCC AAT CC
CISH Exon 2 Splice Donor forward	AAT TAG CTG GGG TAA CCA AT
CISH Exon 2 Splice Donor reverse	CCT TCT AGA CCT CGT CCT TT
TIGIT Exon 1 Splice Donor forward	GTC TGC AAA GTC CTT CAT CT
TIGIT Exon 1 Splice Donor reverse	ATA TGG TTT TTG CCA AAC TT
KLRG1 Exon 4 Splice Donor forward	CCC AAA CAG CAG AAG AAT TA
KLRG1 Exon 4 Splice Donor reverse	TAG GAA TCC AAT GTG GAA AG
PD-1 Exon 1 Splice Donor forward	ACC CTC CCT TCA ACC TGA CC
PD-1 Exon 1 Splice Donor reverse	AAG CCA CAC AGC TCA GGG TA
CD16A S197P mutation forward	TAA AGG ATA TAC GAG ATT AA
CD16A S197P mutation reverse	AAC TGG GTA ATT TAT AAC

Antibodies and flow cytometry

The following antibodies and dyes were used: allophycocyanin (APC)-conjugated, fluorescein isothiocyanate (FITC)-conjugated, or BV650-conjugated anti-CD56 (clone 5.1H11, BioLegend; clone REA196, Miltenyi Biotec; or clone HCD56, BioLegend), FITC-conjugated anti-CD3 (clone OKT3; BioLegend), PE/Cy7-conjugated anti-PD-1 (clone EH12.2H7; BioLegend), eFluor 450-conjugated or Alexa Fluor 700-conjugated anti-TIGIT (clone MBSA43; eBioscience), PE/Dazzle 594-conjugated or FITC-conjugated anti-human CD45 (clone 14C2A07, BioLegend; clone SA231A2, BioLegend), PE/Cy7 anti-human CD16 (clone 3G8, BioLegend), BV421-conjugated anti-human CD45 (clone 2D1; BioLegend), BV605-conjugated anti-mouse CD45 (clone 30-F11; BioLegend), Brilliant violet 421-conjugated anti-IFNγ (clone 4S.B3; BioLegend), Alexa Fluor 700-conjugated anti-TNF-α (clone MAb11; BioLegend), PE-conjugated anti-CD34 (clone QBEnd-10, Invitrogen), APC-conjugated anti-PD-L1 (clone B7-H1, BioLegend), FITC-conjugated anti-CD155 (clone SKII.4, BioLegend), FITC-conjugated anti-DNAM-1 (clone 11A8, BioLegend), Brilliant violet 510-conjugated anti-CD161 (clone HP-3G10, BioLegend), PE/Cyanine7-conjugated anti-Tim3 (clone F38-2E2, BioLegend), APC-conjugated anti-NKG2D (clone 1D11, BioLegend), PE-conjugated anti-NKG2A (clone S19004C, BioLegend), Alexa Fluor 700-conjugated anti-NKp46 (clone 9E2, BioLegend), PE/Dazzle 594-conjugated anti-NKp30 (clone P30-15, BioLegend), FITC-conjugated anti-CD107a (clone H4A3; BD Biosciences), SYTOX Blue dead cell stain (Thermo Fisher), Fixable viability dye eFluor 780 (eBioscience). Flow cytometry was performed on a CytoFLEX S flow cytometer (Beckman Coulter) and all data were analyzed using FlowJo V.10.4 software (FlowJo LLC).

Immunoblotting assay

Proteins were isolated from 1E6 cells in complete radioimmunopercipitation assay (RIPA) buffer with protease and phosphatase inhibitors (Sigma-Aldrich, St Louis, Missouri, USA). Total protein was quantified using the Pierce BCA Protein Assay Kit (Thermo Fisher, Waltham, Massachusetts, USA) according to the manufacturer's protocol. 3 µg/µL of cell lysate was run and analyzed on the Wes platform after being denatured at 95°C for 5 min according to the manufacturer's protocol (ProteinSimple, San Jose, California, USA). Primary antibodies against CISH (Cell Signaling #8731), AhR (Cell Signaling #83200) and beta-actin (Cell Signaling #3700) were all used at 1:50 dilutions in kit-supplied buffer and platform-optimized secondary antibodies were purchased from ProteinSimple.

NK cell intracellular cytokine staining assay

Activated NK cells were plated at 1E6 cells/mL in NK cell medium without cytokines. After incubation overnight, the Burkitt's Lymphoma cell line Raji or T-cell leukemia cell line Jurkat was added at an E:T ratio of 1:1. FITC-conjugated anti-CD107a was added to the culture and cells were incubated for 1 hour at 37°C. Brefeldin A and monensin (BD Biosciences, San Jose, California, USA) were added and cells were incubated for 4 hours. Cells were stained with fixable viability dye, then for extracellular antigens. Cells were fixed and permeabilized using BD Cytofix/Cytoperm (BD Biosciences, San Jose, California, USA) following manufacturer's instructions. Cells were then stained for intracellular IFN-γ and/or TNF-α and analyzed by flow cytometry.

NK cell cytotoxicity assays

Cancer cell lines were seeded into a black round-bottom 96-well plate (5E4 cells per well). NK cells were added to the wells in triplicate at the indicated E:T ratios. Target cells without effectors served as a negative control (spontaneous cell death) and target cells incubated with 1% Triton X-100 served as a positive control (maximum killing). Co-cultures were incubated at 37°C for 48 hours. After incubation, D-luciferin (potassium salt; Gold Biotechnology, St Louis, Missouri, USA) was added to each well at a final concentration of 25 ug/mL and incubated for 5 min with gentle shaking. Luminescence was read in endpoint mode using a BioTek Synergy microplate reader. For *in vitro* killing assays, percent CAR expression was equalized across groups using matched NK cells (for CD19 CAR only groups) or TPC^{KO} NK cells (for codelivery groups), before co-culture set up.

Antibody-dependent cellular cytotoxicity assay

CD20+Raji cells were pretreated with anti-hCD20 mAb (InvivoGen, San Diego, California, USA) at 10 µg/mL for 30 min at 37°C, washed with PBS, and seeded into a black round-bottom 96-well plate (5E4 cells per well). NK cells were added to the wells in triplicate at the indicated E:T ratios. Co-cultures were incubated at 37°C for 4 hours. After incubation, D-luciferin (potassium salt; Gold Biotechnology, St Louis, Missouri, USA) was added to each well at a final concentration of 25 ug/mL and incubated for 5 min with gentle shaking. Luminescence was read in endpoint mode using a BioTek Synergy microplate reader.

CAR construct design

The sequence of the plasmids encoding for CAR and CAR15 is provided in the online supplemental materials.

Droplet digital polymerase chain reaction: copy number analysis

Targeted integration of CAR or CAR15 transposon was quantified using ddPCR. Assays were designed using PrimerQuest software (Integrated DNA Technologies, Coralville, Iowa, USA) using settings for two primers+probe qPCR. Each sample was run as a duplexed assay consisting of an internal reference primer+probe set (RNAseP target, HEX) and an experimental primer+probe set (MND target, FAM), as we previously published. Reactions were set up in duplicate using the ddPCR Supermix for Probes (no dUTP) (Bio-Rad, Hercules, California, USA) with 200 ng genomic DNA per assay according to the manufacturer's instructions. Droplets were generated and analyzed using the QX200 Droplet Digital PCR system (Bio-Rad, Hercules, California, USA).

Droplet digital PCR: translocation studies

Translocation PCR assays were designed using PrimerQuest software (Integrated DNA Technologies, Coralville, Iowa, USA) using settings for 2 primers+probe qPCR from custom designed translocation maps. Each sample was run as a duplexed assay consisting of an internal reference primer+probe set (RNaseP target, HEX, as previously described) and an experimental primer+probe set (FAM). Primers and probes were ordered from IDT. Reactions were set up using the ddPCR Supermix for Probes (no dUTP) (Bio-Rad, Hercules, California, USA) with 200 ng of genomic DNA per assay according to manufacturer's instructions. Droplets were generated and analyzed using the QX200 Droplet-digital PCR system (Bio-Rad, Hercules, California, USA). Frequency was calculated as fractional abundance adjusted for two copies of reference sequence (RNAse P) per genome using the QuantaSoft V.14.0 software (Bio-Rad, Hercules, California, USA).

Primer/Probe name	Sequence
CISH forward	CAG ACA GAG AGT GAG CCA AAG
CISH reverse	CAA ATC AGA CTC AAA GGC AGA AC
CISH probe	TTG GCT ATG CAC AGC AGA TCC TCC
TIGIT forward	CTA CTT TCA GTG GCA GAA GAG G
TIGIT reverse	TAC ACA AGC ACC CAA GTC TC
TIGIT probe	CAC ATC TGC TTC CTG TAG GCC CTC
PD-1 forward	GCT CCA GGC ATG CAG AT
PD-1 reverse	AGG GAC TGA GGG TGG AAG
PD-1 probe	TCG TCT GGG CGG TGC TAC AA

Transposon integration sequencing

Genomic DNA was isolated from engineered CAR-NK cells as previously described.[100] Briefly, sequencing libraries were prepared from 150 ng genomic DNA quantified by Picogreen (Life Technologies) using the Lotus DNA Library Prep Kit (Integrated DNA Technologies) according to the manufacturer's specifications for libraries undergoing target enrichment. Ligations used vendor-supplied "stubby" adapters, with sample-specific 8 bp unique dual indices added during final library amplification. Hybridization capture was performed per manufacturer's protocol with up to 16 libraries in multiplex (500 ng per library) using xGen universal blocking

oligos (IDT) and a custom biotinylated xGen oligo probe pool designed to hybridize to the inserted transposon sequence. Given the small probe panel size, hybridizations and temperature-sensitive washes were performed at 63°C and the total hybridization time was increased from 4 hours to 16 hours. Captured libraries were then amplified to ≥2 nM using KAPA HiFi HotStart 2X PCR master mix, quantified by Picogreen, sized on an Agilent TapeStation using the D1000 assay, normalized, and pooled for 150 bp paired-end sequencing on an Illumina NovaSeq* SP flow cell.

Transposon integration analysis

We analyzed integration site data for *TcBuster* and compared results to published literature data for integration sites of other transposase and viral systems as previously described.[100] Specifically, comparison sequencing datasets were generated by outside sources using different experimental methods. Raw reads from comparison datasets were retrieved (Accession IDs: Lentivirus: SAMN11351981, SAMN11351982, SAMN11351983, SAMN11351984, SAMN00188192, SAMN00188193; Sleeping Beauty: SAMN02870102; and PiggyBac: SAMN02870101) and computationally mapped and analyzed in the same manner as the in-house generated data using Python (V.3.7.10, run on CentOS V.7 Linux).

rhAMPseq off-target analysis

Genomic DNA was purified, and concentration verified using JetSeq Library Quantification Lo-Rox kit (BIO 68029—Meridian BioScience—Memphis, Tennessee, USA) and Quant-iT PicoGreen (p7589—Invitrogen—Carlsbad, California, USA). The NGS library was prepared using the rhAmpSeq CRISPR Library Kit (cat #10007318—Integrated DNA Technologies—Coralville, Iowa, USA). All samples were treated in each protocol as recommended by the manufacturer. Briefly, 50 ng of genomic DNA was added to the Targeted rhAmp PCR 1 which contains rhAmpSeq CRISPR forward and reverse pools. The post-PCR1 product was 1:20 diluted and added to Indexing PCR 2 using Illumina Nextera XT primers (Illumina—San Diego, California, USA). Finally, libraries were pooled and purified with AMPure XP beads (Beckman Coulter—Indianapolis, Indiana, USA). Sequencing was performed using Illumina MiSeq 2X300 paired-end read length (Illumina—San Diego, California, USA).

Sequencing reads were then analyzed using CRISPRessoPooled.[101] First, reads were aligned to the hg38 genome in genome-only mode using the command CRISPRessoPooled -x genome/hg38 -r1 fastq.r1.fq -r2 fastq.r2.fq. The genomic sequences of highly covered regions were extracted from the REPORT_READS_ALIGNED_TO_GENOME_ALL_DEPTHS.txt output file and used to assign gRNA on-targets and off-targets to genomic regions and create a highly-covered-regions.txt region file containing amplicons and their associated gRNA sequence. Next, sequencing reads were reanalyzed with CRISPRessoPooled in genome-and-amplicons mode using the command CRISPRessoPooled -x genome/hg38 -f highly-covered-regions.txt -r1 fastq.r1.fq -r2 fastq.r2.fq. For each region, CRISPResso outputs included counts of reads containing each nucleotide or indels at every position (Nucleotide_frequency_table.txt and Modification_count_vectors.txt). These data were used to calculate the maximum A>G, C>T, and indel rates at positions 3–17 of the gRNA spacer sequence.

In vivo study design

Specific pathogen-free female NSG mice were purchased from The Jackson Laboratory (RRID:IMSR_JAX:005557). Tumor challenge studies were performed using the Raji-luc CD155hi/PD-L1hi cell line. Specifically, mice were implanted with 1E5 Raji cells resuspended in PBS and delivered in 100 µL via tail vein. For the first animal study, 2 days post-tumor implantation, the mice were randomized into treatment groups (n=5) and received either PBS, 5E6 of non-engineered (control) NK cells, CAR NK cells, CAR15 NK cells, CTP^{KO} NK cells, CAR/CTP^{KO} NK cells, or CAR15/CTP^{KO} NK cells the next day. For the second study, 2 days post-tumor implantation, the mice were randomized into treatment groups and received either PBS (n=5), 5E6 of non-engineered (control) NK cells (n=5), CAR15 NK cells (n=10), or CAR15/CTP^{KO} NK cells (n=10) the next day. The same NK cell therapy treatment was repeated 14 days later. For each group, all tumor growth was monitored by weekly bioluminescence imaging of mice 5 min post intraperitoneal injection of D-luciferin (100 µL total volume, 28 mg/kg) using an IVIS Spectrum *in vivo* imaging system followed by region of interest (ROI) analysis of tumor images (Living Image software, V.4.7.3). NK cell persistence in PB was monitored by weekly submandibular blood collection. Endpoint criteria are either mouse paralysis or >20% wt loss within a week. At the endpoint, PB, spleen, and BM were collected and processed to single cell suspensions through standard mashing and ACK-processing and stained for phenotyping markers. This study was carried out in strict accordance with the recommendations in the Guide for the Care and Use of Laboratory Animals of the National Institutes of Health. The protocol and all procedures were approved by the University of Minnesota Institutional Animal Care and Use Committee (Protocol #2110–39527A). The health of the mice was monitored daily by University of Minnesota veterinary staff. The animal research: reporting of in vivo experiments (ARRIVE) reporting guidelines were used for this *in vivo* study.[102]

Statistical analysis

The Student's t-test was used to evaluate the significance of differences between the two groups. Differences between three or more groups with one data point were evaluated by a one-way analysis of variance (ANOVA) test. Differences between three or more groups with multiple data points were evaluated by a two-way ANOVA test.

Differences between groups in our *in vivo* study were evaluated by the Log-rank (Mantel-Cox) test. The level of significance was set at α=0.05. All statistical analyses were performed using GraphPad Prism V.9.2.0.

Author affiliations
[1]Department of Pediatrics, University of Minnesota, Minneapolis, Minnesota, USA
[2]Masonic Cancer Center, University of Minnesota, Minneapolis, Minnesota, USA
[3]Center for Genome Engineering, University of Minnesota, Minneapolis, Minnesota, USA
[4]Department of Genetics, Cell Biology and Development, University of Minnesota, Minneapolis, Minnesota, USA
[5]Department of Biomedical Informatics, The University of Utah, Salt Lake City, Utah, USA

Present affiliations The present affiliation of Mitchell G Kluesner is: Molecular and Cellular Biology Graduate Program, Fred Hutchinson Cancer Center, Seattle, Washington, USA.

Contributors Conceptualization: MW, MGK, EJP, J-WC. Methodology: MW, AKG, EMS, WSL, KL, J-WC. Investigation: MW, JBK, NJS, PNCV, YZ, EJE. Visualization: MW, JBK, JS, JB, KC. Supervision: MW, BM, BRW. Writing—original draft: MW. Writing—review and editing: MW, JS, NJS, EJE, BM, BRW. Guarantor: BM.

Funding National Institutes of Health grant R01AI146009 (BM); National Institutes of Health grant R01AI161017 (BM); National Institutes of Health grant P01CA254849 (BM, BRW); National Institutes of Health grant P50CA136393 (BM, BRW); National Institutes of Health grant U24OD026641 (BM); National Institutes of Health grant P30CA077598 (BM); National Institutes of Health grant U54CA268069 (BM, BRW); National Institutes of Health grant R21CA237789 (BRW); National Institutes of Health grant R21AI163731 (BRW, BM); Hematology Research Training Program T32HL007062-46 (JS); Children's Cancer Research Fund (BM, BRW); The Fanconi Anemia Research Fund (BM, BRW); The Randy Shaver Cancer Research and Community Fund (BM, BRW); Alex's Lemonade Stand Foundation (BRW); Rein in Sarcoma (BRW).

Competing interests MW, EJP, MGK, BM and BRW have filed patents covering the methods and approaches outlined in this work. All other authors declare they have no competing interests.

Patient consent for publication Not applicable.

Ethics approval Not applicable.

Provenance and peer review Not commissioned; externally peer reviewed.

Data availability statement All data relevant to the study are included in the article or uploaded as supplementary information.

ORCID iDs
Minjing Wang http://orcid.org/0000-0003-4725-8351
Joshua B Krueger http://orcid.org/0009-0002-7658-149X
Joseph G Skeate http://orcid.org/0000-0002-1765-5949
Jason B Bell http://orcid.org/0000-0003-4869-6476
Kendell Clement http://orcid.org/0000-0003-3808-0811

REFERENCES

1 Ruggeri L, Capanni M, Urbani E, *et al*. Effectiveness of donor natural killer cell alloreactivity in mismatched hematopoietic transplants. *Science* 2002;295:2097–100.
2 Pan K, Farrukh H, Chittepu V, *et al*. CAR race to cancer immunotherapy: from CAR T, CAR NK to CAR macrophage therapy. *J Exp Clin Cancer Res* 2022;41:119.
3 Suck G, Odendahl M, Nowakowska P, *et al*. NK-92: an "off-the-shelf therapeutic" for adoptive natural killer cell-based cancer immunotherapy. *Cancer Immunol Immunother* 2016;65:485–92.
4 Miller JS, Lanier LL. Natural Killer Cells in Cancer Immunotherapy. *Annu Rev Cancer Biol* 2019;3:77–103.
5 Judge SJ, Murphy WJ, Canter RJ. Characterizing the Dysfunctional NK Cell: Assessing the Clinical Relevance of Exhaustion, Anergy, and Senescence. *Front Cell Infect Microbiol* 2020;10:49.
6 Gong Y, Klein Wolterink RGJ, Wang J, *et al*. Chimeric antigen receptor natural killer (CAR-NK) cell design and engineering for cancer therapy. *J Hematol Oncol* 2021;14:73.
7 Gurney M, O'Reilly E, Corcoran S, *et al*. Concurrent transposon engineering and CRISPR/Cas9 genome editing of primary CLL-1 chimeric antigen receptor–natural killer cells. *Cytotherapy* 2022;24:1087–94.
8 Bexte T, Botezatu L, Miskey C, *et al*. Engineering of potent CAR NK cells using non-viral Sleeping Beauty transposition from minimalistic DNA vectors. *Mol Ther* 2024;32:2357–72.
9 Du Z, Ng YY, Zha S, *et al*. piggyBac system to co-express NKG2D CAR and IL-15 to augment the *in vivo* persistence and anti-AML activity of human peripheral blood NK cells. *Mol Ther Methods Clin Dev* 2021;23:582–96.
10 Skeate JG, Pomeroy EJ, Slipek NJ, *et al*. Evolution of the clinical-stage hyperactive TcBuster transposase as a platform for robust non-viral production of adoptive cellular therapies. *Mol Ther* 2024;32:1817–34.
11 Ma S, Caligiuri MA, Yu J. Harnessing IL-15 signaling to potentiate NK cell-mediated cancer immunotherapy. *Trends Immunol* 2022;43:833–47.
12 Rosenberg SA, Lotze MT, Muul LM, *et al*. Observations on the Systemic Administration of Autologous Lymphokine-Activated Killer Cells and Recombinant Interleukin-2 to Patients with Metastatic Cancer. *N Engl J Med* 1985;313:1485–92.
13 Rosenberg SA. The development of new immunotherapies for the treatment of cancer using interleukin-2. A review. *Ann Surg* 1988;208:121–35.
14 Lodolce JP, Burkett PR, Koka RM, *et al*. Regulation of lymphoid homeostasis by interleukin-15. *Cytokine Growth Factor Rev* 2002;13:429–39.
15 Suck G, Koh MBC. Emerging natural killer cell immunotherapies: large-scale ex vivo production of highly potent anticancer effectors. *Hematol Oncol Stem Cell Ther* 2010;3:135–42.
16 Suck G, Oei VYS, Linn YC, *et al*. Interleukin-15 supports generation of highly potent clinical-grade natural killer cells in long-term cultures for targeting hematological malignancies. *Exp Hematol* 2011;39:904–14.
17 Conlon KC, Lugli E, Welles HC, *et al*. Redistribution, hyperproliferation, activation of natural killer cells and CD8 T cells, and cytokine production during first-in-human clinical trial of recombinant human interleukin-15 in patients with cancer. *J Clin Oncol* 2015;33:74–82.
18 Waldmann TA, Dubois S, Miljkovic MD, *et al*. IL-15 in the Combination Immunotherapy of Cancer. *Front Immunol* 2020;11:868.
19 Zhou Y, Husman T, Cen X, *et al*. Interleukin 15 in Cell-Based Cancer Immunotherapy. *IJMS* 2022;23:7311.
20 Christodoulou I, Ho WJ, Marple A, *et al*. Engineering CAR-NK cells to secrete IL-15 sustains their anti-AML functionality but is associated with systemic toxicities. *J Immunother Cancer* 2021;9:e003894.
21 Liu E, Marin D, Banerjee P, *et al*. Use of CAR-Transduced Natural Killer Cells in CD19-Positive Lymphoid Tumors. *N Engl J Med* 2020;382:545–53.
22 Liu E, Tong Y, Dotti G, *et al*. Cord blood NK cells engineered to express IL-15 and a CD19-targeted CAR show long-term persistence and potent antitumor activity. *Leukemia* 2018;32:520–31.
23 Pomeroy EJ, Hunzeker JT, Kluesner MG, *et al*. A Genetically Engineered Primary Human Natural Killer Cell Platform for Cancer Immunotherapy. *Mol Ther* 2020;28:52–63.
24 Naeimi Kararoudi M, Dolatshad H, Trikha P, *et al*. Generation of Knock-out Primary and Expanded Human NK Cells Using Cas9 Ribonucleoproteins. *J Vis Exp* 2018:58237.

25 Bexte T, Alzubi J, Reindl LM, *et al*. CRISPR-Cas9 based gene editing of the immune checkpoint NKG2A enhances NK cell mediated cytotoxicity against multiple myeloma. *Oncoimmunology* 2022;11:2081415.
26 Mohammadian Gol T, Kim M, Sinn R, *et al*. CRISPR-Cas9-Based Gene Knockout of Immune Checkpoints in Expanded NK Cells. *Int J Mol Sci* 2023;24:16065.
27 Nakazawa T, Morimoto T, Maeoka R, *et al*. CIS deletion by CRISPR/Cas9 enhances human primary natural killer cell functions against allogeneic glioblastoma. *J Exp Clin Cancer Res* 2023;42:205.
28 Webber BR, Lonetree C-L, Kluesner MG, *et al*. Highly efficient multiplex human T cell engineering without double-strand breaks using Cas9 base editors. *Nat Commun* 2019;10:5222.
29 Komor AC, Kim YB, Packer MS, *et al*. Programmable editing of a target base in genomic DNA without double-stranded DNA cleavage. *Nature New Biol* 2016;533:420–4.
30 Gaudelli NM, Komor AC, Rees HA, *et al*. Programmable base editing of A•T to G•C in genomic DNA without DNA cleavage. *Nature New Biol* 2017;551:464–71.
31 Rees HA, Liu DR. Base editing: precision chemistry on the genome and transcriptome of living cells. *Nat Rev Genet* 2018;19:770–88.
32 Kantor A, McClements ME, MacLaren RE. CRISPR-Cas9 DNA Base-Editing and Prime-Editing. *Int J Mol Sci* 2020;21:6240.
33 Richter MF, Zhao KT, Eton E, *et al*. Phage-assisted evolution of an adenine base editor with improved Cas domain compatibility and activity. *Nat Biotechnol* 2020;38:883–91.
34 Liu X, Zhang Y, Cheng C, *et al*. CRISPR-Cas9-mediated multiplex gene editing in CAR-T cells. *Cell Res* 2017;27:154–7.
35 Kuscu C, Parlak M, Tufan T, *et al*. CRISPR-STOP: gene silencing through base-editing-induced nonsense mutations. *Nat Methods* 2017;14:710–2.
36 Dang L, Li G, Wang X, *et al*. Comparison of gene disruption induced by cytosine base editing-mediated iSTOP with CRISPR/Cas9-mediated frameshift. *Cell Prolif* 2020;53:e12820.
37 Zhu H, Blum RH, Bernareggi D, *et al*. Metabolic Reprograming via Deletion of CISH in Human iPSC-Derived NK Cells Promotes In Vivo Persistence and Enhances Anti-tumor Activity. *Cell Stem Cell* 2020;27:224–37.
38 Kluesner MG, Lahr WS, Lonetree C-L, *et al*. CRISPR-Cas9 cytidine and adenosine base editing of splice-sites mediates highly-efficient disruption of proteins in primary and immortalized cells. *Nat Commun* 2021;12:2437.
39 Myers JA, Miller JS. Exploring the NK cell platform for cancer immunotherapy. *Nat Rev Clin Oncol* 2021;18:85–100.
40 Trikha P, Moseman JE, Thakkar A, *et al*. Defining the AHR-regulated transcriptome in NK cells reveals gene expression programs relevant to development and function. *Blood Adv* 2021;5:4605–18.
41 Bai R, Cui J. Burgeoning Exploration of the Role of Natural Killer Cells in Anti-PD-1/PD-L1 Therapy. *Front Immunol* 2022;13:886931.
42 Rousseau A, Parisi C, Barlesi F. Anti-TIGIT therapies for solid tumors: a systematic review. *ESMO Open* 2023;8:101184.
43 Saito M, Suzuki H, Asano T, *et al*. KLMab-1: An Anti-human KLRG1 Monoclonal Antibody for Immunocytochemistry. *Monoclon Antib Immunodiagn Immunother* 2022;41:279–84.
44 Kluesner MG, Nedveck DA, Lahr WS, *et al*. EditR: A Method to Quantify Base Editing from Sanger Sequencing. *The CRISPR Journal* 2018;1:239–50.
45 Benson DM Jr, Bakan CE, Mishra A, *et al*. The PD-1/PD-L1 axis modulates the natural killer cell versus multiple myeloma effect: a therapeutic target for CT-011, a novel monoclonal anti-PD-1 antibody. *Blood* 2010;116:2286–94.
46 MacFarlane AW 4th, Jillab M, Plimack ER, *et al*. PD-1 expression on peripheral blood cells increases with stage in renal cell carcinoma patients and is rapidly reduced after surgical tumor resection. *Cancer Immunol Res* 2014;2:320–31.
47 Beldi-Ferchiou A, Lambert M, Dogniaux S, *et al*. PD-1 mediates functional exhaustion of activated NK cells in patients with Kaposi sarcoma. *Oncotarget* 2016;7:72961–77.
48 Liu Y, Cheng Y, Xu Y, *et al*. Increased expression of programmed cell death protein 1 on NK cells inhibits NK-cell-mediated anti-tumor function and indicates poor prognosis in digestive cancers. *Oncogene* 2017;36:6143–53.
49 Pesce S, Greppi M, Tabellini G, *et al*. Identification of a subset of human natural killer cells expressing high levels of programmed death 1: A phenotypic and functional characterization. *J Allergy Clin Immunol* 2017;139:335–46.
50 Vari F, Arpon D, Keane C, *et al*. Immune evasion via PD-1/PD-L1 on NK cells and monocyte/macrophages is more prominent in Hodgkin lymphoma than DLBCL. *Blood* 2018;131:1809–19.
51 Tumino N, Martini S, Munari E, *et al*. Presence of innate lymphoid cells in pleural effusions of primary and metastatic tumors: Functional analysis and expression of PD-1 receptor. *Intl Journal of Cancer* 2019;145:1660–8.
52 Pesce S, Belgrano V, Greppi M, *et al*. Different Features of Tumor-Associated NK Cells in Patients With Low-Grade or High-Grade Peritoneal Carcinomatosis. *Front Immunol* 1963;10.
53 Quatrini L, Mariotti FR, Munari E, *et al*. The Immune Checkpoint PD-1 in Natural Killer Cells: Expression, Function and Targeting in Tumour Immunotherapy. *Cancers (Basel)* 2020;12:3285.
54 Opitz CA, Litzenburger UM, Sahm F, *et al*. An endogenous tumour-promoting ligand of the human aryl hydrocarbon receptor. *Nature New Biol* 2011;478:197–203.
55 Bernard P-L, Delconte R, Pastor S, *et al*. Targeting CISH enhances natural cytotoxicity receptor signaling and reduces NK cell exhaustion to improve solid tumor immunity. *J Immunother Cancer* 2022;10:e004244.
56 Yusubalieva GM, Dashinimaev EB, Gorchakov AA, *et al*. Enhanced Natural Killers with CISH and B2M Gene Knockouts Reveal Increased Cytotoxicity in Glioblastoma Primary Cultures. *Mol Biol* 2022;56:770–9.
57 Sarhan D, Cichocki F, Zhang B, *et al*. Adaptive NK Cells with Low TIGIT Expression Are Inherently Resistant to Myeloid-Derived Suppressor Cells. *Cancer Res* 2016;76:5696–706.
58 Rishiq A, Bsoul R, Pick O, *et al*. Studying TIGIT activity against tumors through the generation of knockout mice. *Oncoimmunology* 2023;12:2217735.
59 Hasan MF, Campbell AR, Croom-Perez TJ, *et al*. Knockout of the inhibitory receptor TIGIT enhances the antitumor response of ex vivo expanded NK cells and prevents fratricide with therapeutic Fc-active TIGIT antibodies. *J Immunother Cancer* 2023;11:e007502.
60 Hsu J, Hodgins JJ, Marathe M, *et al*. Contribution of NK cells to immunotherapy mediated by PD-1/PD-L1 blockade. *J Clin Invest* 2018;128:4654–68.
61 Pesce S, Greppi M, Grossi F, *et al*. PD/1-PD-Ls Checkpoint: Insight on the Potential Role of NK Cells. *Front Immunol* 2019;10:1242.
62 Sivori S, Vacca P, Del Zotto G, *et al*. Human NK cells: surface receptors, inhibitory checkpoints, and translational applications. *Cell Mol Immunol* 2019;16:430–41.
63 Khan M, Arooj S, Wang H. NK Cell-Based Immune Checkpoint Inhibition. *Front Immunol* 2020;11:167.
64 Ito M, Maruyama T, Saito N, *et al*. Killer cell lectin-like receptor G1 binds three members of the classical cadherin family to inhibit NK cell cytotoxicity. *J Exp Med* 2006;203:289–95.
65 Dixon KJ, Wu J, Walcheck B. Engineering Anti-Tumor Monoclonal Antibodies and Fc Receptors to Enhance ADCC by Human NK Cells. *Cancers (Basel)* 2021;13:312.
66 Wu J, Mishra HK, Walcheck B. Role of ADAM17 as a regulatory checkpoint of CD16A in NK cells and as a potential target for cancer immunotherapy. *J Leukoc Biol* 2019;105:1297–303.
67 Jing Y, Ni Z, Wu J, *et al*. Identification of an ADAM17 cleavage region in human CD16 (FcγRIII) and the engineering of a non-cleavable version of the receptor in NK cells. *PLoS One* 2015;10:e0121788.
68 Nakano O, Sato M, Naito Y, *et al*. Proliferative activity of intratumoral CD8(+) T-lymphocytes as a prognostic factor in human renal cell carcinoma: clinicopathologic demonstration of antitumor immunity. *Cancer Res* 2001;61:5132–6.
69 Ghebeh H, Mohammed S, Al-Omair A, *et al*. The B7-H1 (PD-L1) T lymphocyte-inhibitory molecule is expressed in breast cancer patients with infiltrating ductal carcinoma: correlation with important high-risk prognostic factors. *Neoplasia* 2006;8:190–8.
70 Abiko K, Mandai M, Hamanishi J, *et al*. PD-L1 on tumor cells is induced in ascites and promotes peritoneal dissemination of ovarian cancer through CTL dysfunction. *Clin Cancer Res* 2013;19:1363–74.
71 Yang C-Y, Lin M-W, Chang Y-L, *et al*. Programmed cell death-ligand 1 expression is associated with a favourable immune microenvironment and better overall survival in stage I pulmonary squamous cell carcinoma. *Eur J Cancer* 2016;57:91–103.
72 Yeo M-K, Choi S-Y, Seong I-O, *et al*. Association of PD-L1 expression and PD-L1 gene polymorphism with poor prognosis in lung adenocarcinoma and squamous cell carcinoma. *Hum Pathol* 2017;68:103–11.
73 Zhao Y, Shi F, Zhou Q, *et al*. Prognostic significance of PD-L1 in advanced non-small cell lung carcinoma. *Medicine (Baltimore)* 2020;99:e23172.
74 Oyama R, Kanayama M, Mori M, *et al*. CD155 expression and its clinical significance in non-small cell lung cancer. *Oncol Lett* 2022;23:166.
75 Zhang D, Liu J, Zheng M, *et al*. Prognostic and clinicopathological significance of CD155 expression in cancer patients: a meta-analysis. *World J Surg Oncol* 2022;20:351.

76 Murakami D, Matsuda K, Iwamoto H, *et al*. Prognostic value of CD155/TIGIT expression in patients with colorectal cancer. *PLoS One* 2022;17:e0265908.
77 Guven H, Konstantinidis KV, Alici E, *et al*. Efficient gene transfer into primary human natural killer cells by retroviral transduction. *Exp Hematol* 2005;33:1320–8.
78 Streltsova MA, Barsov E, Erokhina SA, *et al*. Retroviral gene transfer into primary human NK cells activated by IL-2 and K562 feeder cells expressing membrane-bound IL-21. *J Immunol Methods* 2017;450:90–4.
79 Xie G, Dong H, Liang Y, *et al*. CAR-NK cells: A promising cellular immunotherapy for cancer. *EBioMedicine* 2020;59:102975.
80 Obreht I, Hambach U, Veres D, *et al*. Shift of large-scale atmospheric systems over Europe during late MIS 3 and implications for Modern Human dispersal. *Sci Rep* 2017;7:5848.
81 Li L, Mohanty V, Dou J, *et al*. Loss of metabolic fitness drives tumor resistance after CAR-NK cell therapy and can be overcome by cytokine engineering. *Sci Adv* 2023;9:eadd6997.
82 Philip B, Kokalaki E, Mekkaoui L, *et al*. A highly compact epitope-based marker/suicide gene for easier and safer T-cell therapy. *Blood* 2014;124:1277–87.
83 Elmas E, Saljoughian N, de Souza Fernandes Pereira M, *et al*. CRISPR Gene Editing of Human Primary NK and T Cells for Cancer Immunotherapy. *Front Oncol* 2022;12:834002.
84 Naeimi Kararoudi M, Likhite S, Elmas E, *et al*. Optimization and validation of CAR transduction into human primary NK cells using CRISPR and AAV. *Cell Rep Methods* 2022;2:100236.
85 Huang R-S, Shih H-A, Lai M-C, *et al*. Enhanced NK-92 Cytotoxicity by CRISPR Genome Engineering Using Cas9 Ribonucleoproteins. *Front Immunol* 2020;11:1008.
86 Gründemann C, Schwartzkopff S, Koschella M, *et al*. The NK receptor KLRG1 is dispensable for virus-induced NK and CD8+ T-cell differentiation and function in vivo. *Eur J Immunol* 2010;40:1303–14.
87 Jonjic S. Functional plasticity and robustness are essential characteristics of biological systems: lessons learned from KLRG1-deficient mice. *Eur J Immunol* 2010;40:1241–3.
88 Mariotti FR, Petrini S, Ingegnere T, *et al*. PD-1 in human NK cells: evidence of cytoplasmic mRNA and protein expression. *Oncoimmunology* 2019;8:1557030.
89 Davis Z, Felices M, Lenvik T, *et al*. Low-density PD-1 expression on resting human natural killer cells is functional and upregulated after transplantation. *Blood Adv* 2021;5:1069–80.
90 Lai P, Rabinowich H, Crowley-Nowick PA, *et al*. Alterations in expression and function of signal-transducing proteins in tumor-associated T and natural killer cells in patients with ovarian carcinoma. *Clin Cancer Res* 1996;2:161–73.
91 Jewett A, Tseng H-C. Tumor induced inactivation of natural killer cell cytotoxic function; implication in growth, expansion and differentiation of cancer stem cells. *J Cancer* 2011;2:443–57.
92 Tachibana R, Harashima H, Ide N, *et al*. Quantitative analysis of correlation between number of nuclear plasmids and gene expression activity after transfection with cationic liposomes. *Pharm Res* 2002;19:377–81.
93 Glover DJ, Leyton DL, Moseley GW, *et al*. The efficiency of nuclear plasmid DNA delivery is a critical determinant of transgene expression at the single cell level. *J Gene Med* 2010;12:77–85.
94 Colamartino ABL, Lemieux W, Bifsha P, *et al*. Efficient and Robust NK-Cell Transduction With Baboon Envelope Pseudotyped Lentivector. *Front Immunol* 2019;10:2873.
95 Micklethwaite KP, Gowrishankar K, Gloss BS, *et al*. Investigation of product-derived lymphoma following infusion of piggyBac-modified CD19 chimeric antigen receptor T cells. *Blood* 2021;138:1391–405.
96 Bishop DC, Clancy LE, Simms R, *et al*. Development of CAR T-cell lymphoma in 2 of 10 patients effectively treated with *piggyBac* -modified CD19 CAR T cells . *Blood* 2021;138:1504–9.
97 Prommersberger S, Reiser M, Beckmann J, *et al*. CARAMBA: a first-in-human clinical trial with SLAMF7 CAR-T cells prepared by virus-free Sleeping Beauty gene transfer to treat multiple myeloma. *Gene Ther* 2021;28:560–71.
98 Pogue AI, Jaber V, Zhao Y, *et al*. Systemic Inflammation in C57BL/6J Mice Receiving Dietary Aluminum Sulfate; Up-Regulation of the Pro-Inflammatory Cytokines IL-6 and TNFα, C-Reactive Protein (CRP) and miRNA-146a in Blood Serum. *J Alzheimers Dis Parkinsonism* 2017;7:403.
99 Newell MK, Villalobos-Menuey E, Schweitzer SC, *et al*. Cellular metabolism as a basis for immune privilege. *J Immune Based Ther Vaccines* 2006;4:1.
100 Wong DP, Roy NK, Zhang K, *et al*. A BAFF ligand-based CAR-T cell targeting three receptors and multiple B cell cancers. *Nat Commun* 2022;13:217.
101 Clement K, Rees H, Canver MC, *et al*. CRISPResso2 provides accurate and rapid genome editing sequence analysis. *Nat Biotechnol* 2019;37:224–6.
102 Kilkenny C, Browne WJ, Cuthill IC, *et al*. Improving bioscience research reporting: the ARRIVE guidelines for reporting animal research. *PLoS Biol* 2010;8:e1000412.